GDL/GMF-02-03

LAMINAR SOOT PROCESSES (LSP)

by

Z. Dai, A.M. El-Leathy, C.H. Kim, S.S. Krishnan, K.-C. Lin, F. Xu and G.M. Faeth

College of Engineering
Department of Aerospace Engineering
The University of Michigan
Ann Arbor, Michigan 48109-2140

GDL/GMF-02-03

LAMINAR SOOT PROCESSES (LSP)

by

Z. Dai,[a] A.M. El-Leathy, C.H. Kim, S.S. Krishnan,[b] K.-C. Lin,[c] F. Xu[d] and G.M. Faeth
Department of Aerospace Engineering
The University of Michigan
Ann Arbor, Michigan 48109-2140

Final Report
1 June 2000-31 October 2002

15 December 2002

NASA Grant No. NAG3-2404
Office of Biological and Physical Research
National Aeronautics and Space Administration
Washington, DC 20546
D.L. Urban and Z.-G. Yuan, NASA Glenn Research Center, Project Scientists

---

[a]Now at G.E. Aircraft Engines, Cincinnati, Ohio.

[b]Now at the University of Indiana and Purdue at Indianapolis, Indiana.

[c]Now at Taitec, Inc., Wright-Patterson Air Force Base, Ohio.

[d]Now at the University of Central Florida, Orlando, Florida.

LAMINAR SOOT PROCESSES (LSP)

This is the final report of a research program considering the structure and the soot surface reaction properties of laminar nonpremixed (diffusion) flames. The study was limited to ground-based measurements of buoyant laminar jet diffusion flames at pressures of 0.1-1.0 atm. The motivation for the research is that soot formation in flames is a major unresolved problem of combustion science that influences the pollutant emissions, durability and performance of power and propulsion systems, as well as the potential for developing computational combustion. The investigation was divided into two phases considering the structure of laminar soot-containing diffusion flames and the soot surface reaction properties (soot surface growth and oxidation) of these flames, in turn.

The first phase of the research addressed flame and soot structure properties of buoyant laminar jet diffusion flames at various pressures. The measurements showed that H, OH and O radical concentrations were generally in superequilibrium concentrations at atmospheric pressure but tended toward subequilibrium concentrations as pressures decreased. The measurements indicated that the original fuel decomposed into more robust compounds at elevated temperatures, such as acetylene (unless the original fuel was acetylene) and H, which are the major reactants for soot surface growth, and that the main effect of the parent fuel on soot surface growth involved its yield of acetylene and H for present test conditions.

The second phase of the research addressed soot surface reaction properties, e.g., soot surface growth and surface oxidation. It was found that soot surface growth rates in both laminar premixed and diffusion flames were in good agreement, that these rates were relatively independent of fuel type, and that these rates could be correlated by the Hydrogen-Abstraction/Carbon-Addition (HACA) mechanisms of Colket and Hall (1994), Frenklach et al. (1990,1994), and Kazakov et al. (1995). It was also found that soot surface oxidation rates were relatively independent of fuel type, were not correlated with O_2, CO_2, H_2O and O collision rates but were correlated with the collision rates of OH with a collision efficiency of 0.14, in agreement with the early measurements in premixed flames of Neoh et al. (1980), after allowing for oxidation by O_2 via the classical rate expression of Nagle and Strickland-Constable (1962).

Acknowledgments

The authors wish to acknowledge the contributions of the staff of the Gas Dynamics Laboratories of the Department of Aerospace Engineering at the University of Michigan as follows: C.J. Chartier, M.J. Etzel, T.C. Griffin, T.M. Larrow and D.J. McLean for help with apparatus development and experiments; and S.C. Bauerle and S.B. Smith for help with communications, financial management and publications. Finally, support of the research by the Office of Biological and Physical Research of NASA, with D.L. Urban and Z.-G. Yuan of the NASA Glenn Research Center serving as Project Scientists, is also very much appreciated.

Table of Contents

List of Tables

List of Figures

Nomenclature

C/O	=	ratio of molar concentrations of carbon to oxygen
C_i	=	mass of carbon oxidized per mole of species i reacted, kg/kgmol
d	=	fuel port exit diameter, m
d_p	=	mean primary soot particle diameter, m
f_s	=	soot volume fraction
Fr	=	burner exit Froude number, $u_o^2/(gd)$
F/O	=	ratio of molar concentrations of fuel to oxygen atoms
g	=	acceleration of gravity, ms^{-2}
[i]	=	molar concentration of species i, kgmole m^{-3}
M_i	=	molecular weight of species i, kg $kgmol^{-1}$
n_p	=	number of primary particles per unit volume, m^{-3}
Re	=	burner exit Reynolds number, $u_o d/\nu_o$
R_i	=	terms in the hydrogen-abstraction/carbon-addition (HACA) soot surface growth rate formulas, $kgm^{-2}s^{-1}$
R_u	=	universal gas constant, $Jkgmol^{-1}K^{-1}$
S	=	soot surface area per unit volume, m^{-1}
t	=	time, s
T	=	temperature, K
u	=	streamwise velocity, ms^{-1}
$\bar{v}_i$	=	mean molecular velocity of species i, ms^{-1}
w_g	=	soot surface growth rate, $kgm^{-2}s^{-1}$
w_{ox}	=	soot surface oxidation rate, $kgm^{-1}s^{-1}$
z	=	streamwise distance, m

Greek Symbols

α_i = steric factor in HACA soot surface growth expression for mechanism i

η_i = collision efficiency of species i

ν = kinematic viscosity, m^2s^{-1}

ρ = gas density, kg m^{-3}

ρ_s = soot density, kg m^{-3}

ϕ = fuel-equivalence ratio

Subscripts

o = burner exit condition

CH = HACA soot surface growth mechanism of Colket and Hall (1994)

FW = HACA soot surface growth mechanism of Frenklach and Wang (1990,1994) and Kazakov et al. (1996)

1. Introduction

A study of soot processes relevant to practical turbulent nonpremixed (diffusion) flames, using laminar flames as model flame systems for both theory and experiment, is described. The findings of the research are relevant to the pollutant and particle emission properties of combustion processes, the radiant head loads of combustors and unwanted fires, the hazards of terrestrial and spacecraft fires, and capabilities for developing computational combustion. The main objective of the research is to develop and interpret a flight experiment for observations of truly steady and nonbuoyant laminar jet diffusion flames at microgravity conditions using Space Shuttle facilities, which is known to be the only experimentally and computationally proper paradigm for soot processes in practical turbulent diffusion flames (Dai and Faeth, 2000; Faeth, 1991, 2001; Law and Faeth, 1994; Liu et al., 1996; Sunderland et al., 1994; Urban et al., 1998, 2000). Ground-based experiments to observe soot processes in both premixed and nonpremixed buoyant laminar flames are also being undertaken in order to support the flight program and to develop an improved understanding of soot formation processes in flame environments. No flight experiments were carried out during this report period, however, so that the present report is limited to consideration of findings of the ground-based program, alone. Descriptions of past results of the flight program can be found in Dai et al. (1997,2000), Faeth (2001), Lin and Faeth (1999), Urban et al. (1998, 2000) and Xu et al. (2003b).

Soot processes in turbulent diffusion flames are of greatest practical interest; nevertheless, direct study of soot processes in turbulent flames is not feasible using either existing or anticipated technology. In particular, the unsteadiness and distortion of turbulent flames limits available temporal and spatial resolution within regions where soot processes are important. As a result, laminar diffusion flames are used as more tractable model flame systems to study soot processes relevant to practical turbulent diffusion flames. This is justified by the known similarities between gas-phase processes in these two flame systems (Bilger, 1997; Faeth, 1997, 2001); unfortunately, buoyant laminar diffusion flames do not have corresponding utility for studying processes of particulate matter like soot in flames, which is one of the reasons why current understanding of soot processes in turbulent diffusion flames is very limited (Faeth, 1991; Law and Faeth, 1994; Dai et al., 1997). The differences between soot processes in buoyant and nonbuoyant laminar jet diffusion flames are mainly due to the different hydrodynamic properties of these flames. The reasons for this behavior are illustrated in Fig. 1, where some features of buoyant and nonbuoyant laminar jet diffusion flames are plotted as a function of position in the flames, as follows: the region bounded by ϕ=1-2 is marked because these conditions are associated with soot formation, and soot pathlines are shown that characterize the motion of soot particles in the flames. The differences between the two flames are striking: in buoyant flames, soot first nucleates near the flame sheet (ϕ=1) and then moves toward fuel-rich conditions for a time before accelerating and being swept back through the

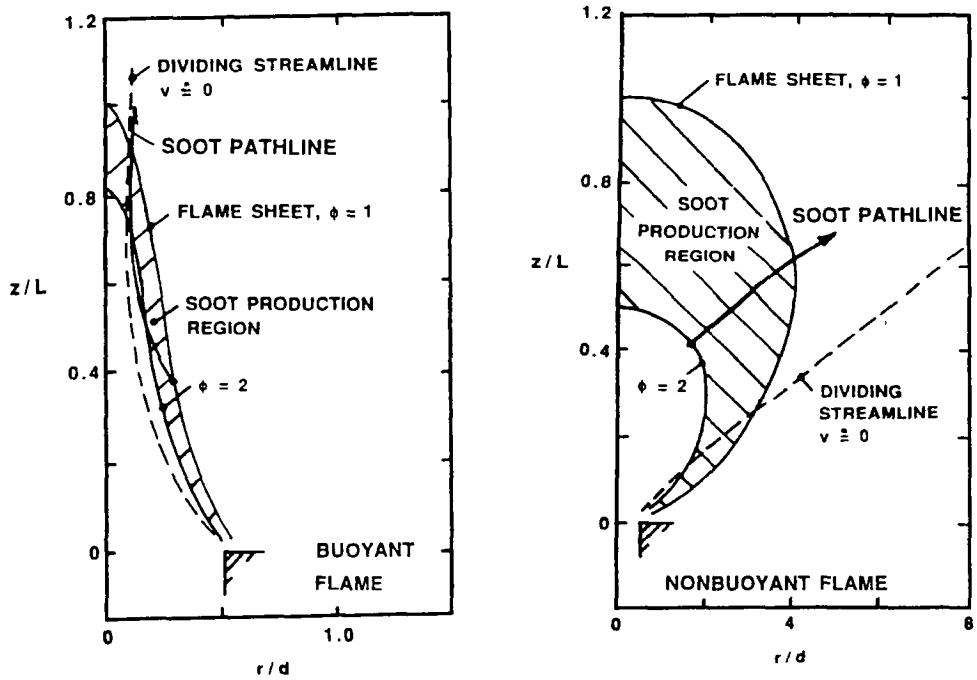

Fig. 1 Sketch of soot paths in buoyant and nonbuoyant laminar jet diffusion flames. From Sunderland et al. (1994).

flame near its tip; in contrast, for nonbuoyant flames, soot first nucleates near the cool core of the flame and then is drawn directly toward and through the flame sheet while continuously decelerating. This implies very different distributions of soot-formation-to-soot-oxidation residence times, and thus, very different soot properties for the two flames, e.g., the laminar smoke point properties of nonbuoyant flames are very different from those of buoyant flames (Sunderland et al., 1994; Urban et al., 2000). Additionally, because local effects of buoyancy generally are insignificant for practical turbulent flames, the proper laminar diffusion flame paradigm for soot processes in practical turbulent diffusion flames is the nonbuoyant diffusion flame (Law and Faeth, 1994). These differences between nonbuoyant and buoyant flames provide considerable motivation for the study of soot processes in nonbuoyant laminar jet diffusion flames at microgravity, as well as the associated ground-based measurements and their analysis of the structure and soot reaction properties of buoyant laminar jet diffusion flames.

The following description of the research is brief. Additional details can be found in the archival publications, the papers, the conference proceedings and the theses resulting from the investigation that are summarized in Table 1. This table also provides a summary of invited and contributed oral presentations of the research results, honors and awards obtained during the grant period and participants in the investigation. Finally, for convenience, several articles resulting from the research during this report period are reproduced in the appendices, including Dai and Faeth (2000), El-Leathy et al. (2003a), Krishnan et al. (2000,2001), Lin and Faeth (2000), Urban et al. (2000), Xu and Faeth (2000,2001) and Xu et al. (2002,2003).

The following report considers ground-based studies of the structure and soot reaction properties of soot-containing laminar jet diffusion flames, treating each topic in turn. Each section is written so that it stands alone; therefore, readers can skip to sections of interest.

Table 1. Summary of Investigation[a]

Archival Publications (articles and book chapters):

Dai, Z. and Faeth, G.M. (2000) "Hydrodynamic Suppression of Soot Formation in Laminar Coflowing Jet Diffusion Flames," *Proc. Combust. Inst.*, 28, 2085-2092.

El-Leathy, A.M., Xu, F., Kim, C.H. and Faeth, G.M., (2003a) "Soot Surface Growth in Laminar Hydrocarbon/Air Diffusion Flames," *AIAA J.*, in press.

El-Leathy, A.M., Kim, C.H., Xu, F. and Faeth, G.M. (2003b) "Structure and Soot Reaction Properties of High-Temperature Diffusion Flames at Atmospheric Pressure," *AIAA J.*, in preparation.

Faeth, G.M. (2001) "Gaseous Laminar and Turbulent Diffusion Flames," *Microgravity Combustion Science* (H.D. Ross, ed.), Academic Press, New York, Chapt. 3, 83-182.

Kim, C.H., El-Leathy, A.M., Xu, F. and Faeth, G.M., " Soot Surface Growth and Oxidation in Diffusion Flames at Subatmospheric and Atmosperic Pressures," *Combust. Flame*, in preparation.

Krishnan, S.S., Lin, K.-C. and Faeth, G.M., (2000) "Optical Properties in the Visible of Overfire Soot in Large Buoyant Turbulent Diffusion Flames," *J. Heat Trans.* 122, 517-524.

Krishnan, S.S., Lin, K.-C. and Faeth, G.M. (2001) "Extinction and Scattering Properties of Soot Emitted from Large Buoyant Turbulent Diffusion Flames," *J. Heat Trans.* 123, 331-339.

Lin, K.-C. and Faeth, G.M. (2000) "State Relationships of Laminar Permanently-Blue Opposed-Jet Hydrocarbon-Fueled Diffusion Flames," *Int. J. Environ. Combust. Tech.* 1, 53-79.

Urban, D.L., Yuan, Z.-G., Sunderland, P.B., Lin, K.-C., Dai, Z. and Faeth, G.M. (2000) "Smoke-Point Properties of Nonbuoyant Round Laminar Jet Diffusion Flames," *Proc. Combust. Inst.* 28, 1965-1972.

Xu, F. and Faeth, G.M. (2000) "Structure of the Soot Growth Region of Laminar Premixed Methane/Oxygen Flames," *Combust. Flame* 121, 640-650

Xu, F. and Faeth, G.M. (2001) "Soot Formation in Laminar Acetylene/Air Diffusion Flames at Atmospheric Pressure," *Combust. Flame* 125, 804-819.

Xu, F., Dai, Z. and Faeth, G.M. (2002) "Flame Shapes of Nonbuoyant Laminar Jet Diffusion Flames," *AIAA J.* 40, 2439-2446.

Xu, F., El-Leathy, A.M., Kim, C.-H. and Faeth, G.M. (2003a) "Soot Surface Oxidation in Laminar Hydrocarbon/Air Diffusion Flames at Atmospheric Pressure," *Combust. Flame*, in press.

Papers and Conference Proceedings:

Dai, Z. and Faeth, G.M. (2000) "Shapes of Nonbuoyant Laminar Jet Diffusion Flames at Soot- and Smoke-Point Conditions," *Proceedings of the Spring Technical Meeting*, Canadian Section of the Combustion Institute, Pittsburgh, 22-1 to 22-6.

Dai, Z. and Faeth, G.M. (2000) "Soot- and Smoke-Point Properties of Laminar Coflowing Jet Diffusion Flames, *Proceedings of the Spring Technical Meeting*, Central States Section, The Combustion Institute, Pittsburgh, 39-44.

Dai, Z., Xu, F. and Faeth. G.M. (2001) "Shapes of Soot-Free Hydrocarbon/Air Laminar Coflowing Jet Diffusion Flames," *39th AIAA Aerospace Sciences Meeting*, Reno, AIAA Paper No. 2001-1078.

El-Leathy, A.M., Xu, F. and Faeth, G.M. (2001) "Soot Growth in Hydrocarbon-Fueled Laminar Diffusion Flames at Atmospheric Pressure," *39th AIAA Aerospace Sciences Meeting*, Reno, AIAA Paper No. 2001-1077,.

El-Leathy, A.M., Xu, F. and Faeth, G.M. (2001) "Early Soot Oxidation in Hydrocarbon-Fueled Laminar Jet Diffusion Flames at Atmospheric Pressure," *Proceedings of 2nd Joint Meeting of the U.S. Sections*, The Combustion Institute, Pittsburgh, 26.

El-Leathy, A.M., Xu, F. and Faeth, G.M. (2001) "Soot Growth and Oxidation in Laminar Jet Diffusion Flames," *Proceedings of the Spring Technical Meeting*, Canadian Section, The Combustion Institute, Pittsburgh.

El-Leathy, A.M., Xu, F. and Faeth, G.M. (2001) "Structure and Soot Formation Properties of Laminar Diffusion Flames," *6th International Microgravity Combustion Workshop*, NASA/CP-2001-210826, Washington, pp. 325-328.

El-Leathy, A.M., Xu, F. and Faeth, G.M. (2001) "Structure and Early Soot Oxidation Properties of Laminar Diffusion Flames," *6th International Microgravity Combustion Workshop*, NASA/CP-2001-21086, Washington, pp. 169-172.

El-Leathy, A.M., Xu, F. and Faeth, G.M., "Soot Surface Growth and Oxidation in Laminar Unsaturated-Hydrocarbon/Air Diffusion Flames," *40th AIAA Aerospace Sciences Meeting*, Reno, Paper No. 2002-1116.

El-Leathy, A.M., Xu, F., Kim, C.H. and Faeth, G.M. (2001) "Soot Reaction and Flame Structure Properties of Laminar Benzene/Acetylene/Nitrogen-Fueled Laminar Jet Diffusion Flames," *Proceedings of the Fall Technical Meeting*, Eastern Section of the Combustion Institute, Pittsburgh, 219-222.

El-Leathy, A.M., Xu, F., Kim, C.H. and Faeth, G.M. (2002) "Soot Formation and Early Oxidation in Laminar Diffusion Flames at Atmospheric Pressure," *Proceedings of the Spring Technical Meeting*, Central States Section of the Combustion Institute, Pittsburgh.

El-Leathy, A.M., Kim, C.H., Xu, F. and Faeth, G.M. (2003) "Structure and Soot Reaction Properties of High-Temperature Diffusion Flames," *Proceedings of the Third Joint Meeting of the U.S. Sections*, The Combustion Institute, Pittsburgh, in press.

Faeth, G.M. (1999) "Flame-Flow Interactions During Combustion of Gases," *52nd Annual Meeting*, American Physical Society Bulletin, 44, 129 (Abstract only).

Kim, C.H., El-Leathy, A.M., Xu, F. and Faeth, G.M. (2003) "Soot Surface Growth and Oxidation in Diffusion Flames at Subatmospheric and Atmosperic Pressures," *41st AIAA Aerospace Sciences Meeting*, Reno, AIAA Paper No. 2003-0665.

Kim, C.H., El-Leathy, A.M., Xu, F. and Faeth, G.M. (2003) "Structure and Soot Surface Reaction Properties of Laminar Jet Diffusion Flames," *Proceedings of the Spring Technical Meeting*, Canadian Section, The Combustion Institute, Pittsburgh, in press.

Krishnan, S.S., Lin, K.-C. and Faeth, G.M. (2000) "Extinction and Scattering Properties of Soot Emitted from Large Buoyant Turbulent Diffusion Flames," *34th National Heat Transfer Conference*, Pittsburgh, 219-222.

Urban, D.L. and Faeth, G.M. (2001) "Soot Research in Combustion Science: Introduction and Review of Current Work," *39th Aerospace Sciences Meeting*, Reno, Paper No. 2001-0322.

Urban, D.L. and Faeth, G.M. (2002) "Soot Formation and Oxidation in Premixed and Nonpremixed Flame Environments," *Proceedings of the Spring Technical Meeting*, Canadian Section, The Combustion Institute, Pittsburgh.

Urban, D.L. and Faeth, G.M. (2002) "Optical and Reactive Properties of Soot in Flame Environments," *Proceedings of the Spring Technical Meeting*, Central States Section, The Combustion Institute, Pittsburgh.

Xu, F. and Faeth, G.M. (2000) "Soot Reaction and Flame Structure Properties of Laminar Acetylene/Air Diffusion Flames at Atmospheric Pressure," *Proceedings of the Spring Technical Meeting*, Central States Section, The Combustion Institute, Pittsburgh, 11-16.

Xu, F. and Faeth, G.M. (2000) "Soot Growth and Oxidation in Laminar Diffusion Flames," *Proceedings of the Spring Technical Meeting*, Canadian Section of the Combustion Institute, Pittsburgh, 19-1 to 19-6.

Xu, F. and Faeth, G.M. (2000) "Soot Growth in Acetylene/Air Laminar Jet Diffusion Flames at Atmospheric Pressure," Twenty-Eighth Symposium (International) on Combustion, The Combustion Institute, Pittsburgh, poster paper.

Xu, F. and Faeth, G.M. (2001) "Soot and Smoke-Point Properties of Plane Laminar Jet Diffusion Flames," *Proceedings of the Spring Technical Meeting*, The Canadian Section of the Combustion Institute, Pittsburgh.

Xu, F., Dai, Z. and Faeth, G.M. (2001) "Suppression of Soot Formation and Shapes of Laminar Jet Diffusion Flames," *Sixth International Microgravity Combustion Workshop*, NASA/CP-2001-210826, Washington, 173-176,

Theses:

El-Leathy, A.M. (2002) "Effect of Hydrocarbon Fuel Type on Soot Surface Growth and Oxidation in Laminar Diffusion Flames," Ph.D. Thesis, Mechanical Power Department, Helwan University , Cairo, Egypt.

Reports:

Dai, Z., El-Leathy, A.M., Lin, K.-C., Sunderland, P.B., Xu, F., and Faeth, G.M. (2000) "Laminar Soot Processes (LSP)," Report No. GDL/GMF 00-03, Department of Aerospace Engineering, The University of Michigan, Ann Arbor, Michigan.

Oral Presentations (Invited):

Faeth, G.M. (2000) "Laminar Soot Processes (LSP) Science Overview," NASA Glenn Research Center, Cleveland.

Faeth, G.M. (2000) "Combustion Module-2: Laminar Soot Processes," NASA Kennedy Space Center, Cape Canaveral.

Faeth, G.M. (2000) "Laminar Soot Processes (LSP) Overview," Spacehab Corp., Cape Canaveral.

Faeth, G.M. (2001) "Overview of NASA Research in Combustion Science," Space Studies Board, National Research Council, Washington.

Faeth, G.M. (2001) "Soot Formation and Oxidation in Flames: Findings from Ground-Based and Space-Shuttle Experiments," CNES Colloquium on Materials Science in Microgravity, Paris.

Faeth, G.M. (2001) "Micro-G and You: Space Research and Benefits on Earth in Physical Sciences/Combustion," PanPacific Conference on Micro-G, Los Angeles.

Faeth, G.M. (2001) Soot Formation and Oxidation in Flames," LCSR Seminar, University of Orleans, Orleans

Faeth, G.M. (2001) "Structure and Soot Formation Properties of Laminar Flames," 6th International Microgravity Combustion Workshop, NASA Glenn Research Center, Cleveland.

Faeth, G.M. (2001) "Structure and Early Soot Oxidation Properties of Laminar Diffusion Flames," 6th International Microgravity Combustion Workshop, NASA Glenn Research Center, Cleveland.

Faeth, G.M. (2001) "Suppression of Soot Formation and Shapes of Laminar Jet Diffusion Flames," 6th International Microgravity Combustion Workshop, NASA Glenn Research Center, Cleveland

Faeth, G.M. (2001) "Soot Formation and Oxidation in Laminar Premixed and Nonpremixed Flames," XXIV Event of the Italian Section of the Combustion Institute, S. Margherita Ligure.

Faeth, G.M. (2002) "Soot Surface Growth and Oxidation Properties of Premixed and Nonpremixed Flames," Distinguished Lecturer Series, Department of Chemical and Fuels Engineering, University of Utah, Salt Lake City.

Faeth, G.M. (2002) "Optical and Reactive Properties of Soot in Flame Environments," Plenary Lecture, Spring Technical Meeting, Central States Section of the Combustion Institute, Knoxville.

Faeth, G.M. (2002) "Soot Formation and Oxidation in Premixed and Nonpremixed Flame Environments," Plenary Lecture, Spring Technical Meeting, Canadian Section of the Combustion Institute, Windsor.

Oral Presentations (Excluding conference papers that were presented orally):

Faeth, G.M. (2000) "Soot Growth in Acetylene/Air Laminar Jet Diffusion Flames at Atmospheric Pressure," Twenty-Eighth Symposium (International) on Combustion, The Combustion Institute, Pittsburgh.

Honors/Awards:

Faeth, G.M. (2000) Highly-Cited Researcher Certificate (for being among the 99 most-cited engineers in the world),

Faeth, G.M. (2002) Medal of Appreciation, Helwan University, Cairo, Egypt.

Faeth, G.M. (2002) Invited James E. Peters Plenary lecture, "Optical and Radiative Properties of Soot in Flame Environments," Spring Technical Meeting, Central States Section, The Combustion Institute, Knoxville.

Faeth, G.M. (2002) Invited Distinguished Lecturerer Series , Department of Chemical and Fuels Engineering, The University of Utah, Salt Lake City, Utah.

Faeth, G.M. (2002) Invited Plenary Lecture, Spring Technical Meeting, Canadian Section of the Combustion Institute, Windsor, Canada.

Participants:

Dai, Z., Postdoctoral Research Fellow, The University of Michigan, Ann Arbor, Michigan.

El-Leathy, A.M., (1) Visiting Research Scholar, Mechanical Power Department, Helwan University, Cairo, Egypt, and (2) Postdoctoral Research Fellow, The University of Michigan, Ann Arbor, Michigan.

Kim, C.H., Graduate Student Research Assistant (GSRA), The University of Michigan, Ann Arbor, Michigan.

Krishnan, S.S., Graduate Student Research Assistant (GSRA), The University of Michigan, Ann Arbor, Michigan.

Lin, K.-C., Postdoctoral Research Fellow, The University of Michigan, Ann Arbor, Michigan.

Xu, F., Postdoctoral Research Fellow, The University of Michigan, Ann Arbor, Michigan.

[a]For the period 1 June 2000-30 November 2002.

2. Laminar Diffusion Flame Structure

2.1 Introduction

Ground-based studies of the structure and soot processes of laminar flames proceeded in two phases, considering laminar premixed and diffusion flames, in turn. The laminar premixed flames involved round flat flame burners directed vertically upward at atmospheric pressure with coflowing nitrogen used to prevent flame oscillations and with the measurements limited to the flame axes. The measurements were sufficient to resolve soot nucleation and soot surface growth rates, see Table 2 for a summary of the measurements that were made. These results have already been described in Xu et al. (1997), who considered ethylene/air flames similar to Harris and Weiner (1983a,b,1984a,b), and Xu et al. (1998) and Xu and Faeth (2000) who considered methane/oxygen flames similar to Ramer et al. (1986), see Table 3 for a summary of the test conditions considered during the laminar premixed flame experiments. The methods and results of this work are described in the references just mentioned and are summarized in a previous report under the present investigation, e.g., Dai et al. (2000). It was found that predictions of major gas species using the mechanisms of Leung and Lindstedt (1995), Leung et al. (1991) and Frenklach and Wang (1990) were in good agreement with each other, and with the measurements of flame properties; that H-atom concentrations generally satisfy the requirements of local thermodynamic equilibrium within the soot growth region, that soot surface growth rates were independent of fuel type and could be correlated by Hydrogen-Abstraction/Carbon-Addition (HACA) the soot surface growth mechanisms of Frenklach et al. (1990,1994), Kazakov et al. (1995) and Colket and Hall (1994) with steric factors on the order of unity. Given this status, the objectives of the present investigation were to study the structure and soot surface reaction properties of laminar jet diffusion flames considering various hydrocarbons burning in air at pressures of 0.1-1.0 atm.

Table 2. Summary of Experimental Methods

Measurements	Method
Soot volume fraction	Laser extinction[a]
Soot structure	Transmission electron microscopy (TEM)[b]
Soot temperature	Multiline emission[a]
Gas temperature	Extrapolated thermocouples[c]
Gas composition	Gas chromatography
Radical (H, OH, O) composition	Li/LiOH atomic absorption[a]
Flow velocities	Laser velocimetry

[a]Deconvolution measurements for chord-like paths.
[b]Also high resolution transmission electron microscopy (HRTEM).
[c]Extrapolating results for thermocouples having different bead sizes to an infinitely-small bead size.

The test arrangement for the present study of laminar jet diffusion flames involved round fuel ports directed vertically upward, with a coflow of air in order to prevent flame oscillations and with the measurements limited to the flame axes. The measurements were sufficient to resolve soot nucleation , soot surface growth and soot surface oxidation rate properties, see Table 2 for a summary of the measurements that were made. The present discussion of the research is brief, more details can be found in El-Leathy et al. (2003a), Kim et al. (2003), Xu and Faeth (2001), and Xu, et al. (2003a),

Naturally, the present laminar jet diffusion flames were buoyant, which raises questions about the appropriateness of these flames for fundamental studies of their structure and the soot surface reaction properties in view of the discussion associated with Fig. 1. This concern was addressed by only considering flame structure and the soot surface reaction properties along the axes of the flames. For paths along the axes of buoyant laminar flames, soot particles form near the cool core of the flames and are drawn directly toward and through the flame sheet in qualitatively the same manner as for nonbuoyant laminar jet diffusion flames. In addition, the

Table 3. Premixed Flame Test Conditions[a]

Flame	Fuel-Equivalence Ratio	C/O Ratio[b]	F/O Ratio[c]
Ethylene/air flames due to Harris and Weiner (1983a,b,1984a,b) from Xu et al. (1997):			
1	2.34	0.78	---
2	2.49	0.83	---
3	2.64	0.88	---
4	2.79	0.93	---
5	2.94	0.98	---
Methane/oxygen flames similar to Ramer et al. (1986) from Xu et al. (1998):			
6	2.35	---	1.10
7	2.45	---	1.15
8	2.56	---	1.20
9	2.67	---	1.25
10	2.77	---	1.35

[a]Premixed, 60 mm diameter McKenna Products, Inc. water-cooled flat flame burner directed vertically upward at atmospheric pressure with a 6 mm wide annular nitrogen coflow.

[b]Atomic carbon/oxygen (C/O) ratios.

[c]Molar fuel/oxygen flow rate (F/O) ratios.

fact that velocities along the axes nonbuoyant laminar jet diffusion flames decrease with increasing distance from the jet exit whereas those for most buoyant laminar jet diffusion flames increase with increasing distance from the jet exit affects residence times in the flame, however, this effect was quantified during the present study by directly measuring flow velocities along the flame axes.

Activities associated with the present study of the soot-containing laminar jet diffusion flames are described in the following, considering experimental methods, experimental results, and conclusions, in turn.

2.2 Experimental Methods

Two test arrangements were used for the laminar jet diffusion flame studies, one for experiments at atmospheric pressure, and one for experiments at pressures of 0.1-1.0 atm. The atmospheric pressure burner consisted of a 34.8 mm diameter fuel port directed vertically upward, terminated with a honeycomb, and a 60 mm diameter coannular air port for an air coflow in order to eliminate flow oscillations. The burner was not cooled because the flames were somewhat separated from the burner exit. Room disturbances were controlled by surrounding the flames with layers of screens and a plastic enclosure. The combustion products were removed using the laboratory exhaust system. The burner could be traversed in the horizontal and vertical directions in order to accommodate rigidly-mounted optical instrumentation. Experimental methods used for measurements in the diffusion flames were the same as for the premixed flames as discussed in connection with Table 2.

The variable pressure test apparatus was similar to the arrangement used by Sunderland et al. (1995) and Sunderland and Faeth (1996) for measurements of the soot properties of laminar jet diffusion flames at subatmospheric pressures. The arrangement consisted of a round fuel jet having a diameter of 3.3 mm, injected vertically upward and surrounded by a slow concentric flow of air. The flames burned along the axis of a vertical windowed cylindrical chamber having a diameter and length of 300 mm. The top and bottom of the chamber consisted of porous metal plates that separated the flame chamber from plenum chambers for air inflow and exhaust outflow and provided a uniform distribution of air flow over the flow chamber cross section. The combustion products were removed using a vacuum pump. The flames were ignited by a hot wire that could be retracted from the burner exit once ignition was complete. The entire chamber could be traversed in the vertical and horizontal directions in order to accommodate rigidly-mounted optical instruments.

Instrumentation for both diffusion flame test arrangements was the same as for the premixed flame measurements as summarized in Table 2; test conditions for the diffusion flame experiments are summarized in Table 4. The experiments began with the acetylene/air flames at atmospheric pressure considered by Xu and Faeth (2001); this was done because acetylene is a basic building block of soot growth via classical HACA soot growth mechanisms (Frenklach and Wang, 1990,1994; Colket and Hall, 1994). The fuel was diluted with nitrogen for these tests in order to control maximum soot concentrations in the flames so that excessive buildup of soot on instrumentation probes was avoided. Effects of fuel type were considered subsequently for ethylene, propylene and propane, as well as acetylene/benzene mixtures, with all fuels burning in air and again using nitrogen dilution to control soot levels in the flames. In particular, the acetylene/benzene mixtures were used in order to promote the PAH mechanism of soot growth in comparison to the HACA mechanism because the PAH mechanism is advocated as the main mechanism for soot growth, compared to the HACA soot surface growth mechanism, by some workers in the field (Bockhorn et al. 1982,1984; Wieschnowsky et al., 1988; Colket and Hall 1994; Frenklach and Wang, 1990; Maus et al., 1994; Kazakov et al., 1995). Finally, effects of varying pressure were considered using acetylene/air flames, once again using nitrogen dilution to control maximum soot contractions. The low pressure flames in these tests, at 0.125 and 0.250 atm, were similar to diffusion flames considered earlier by Sunderland et al. (1995). The return to acetylene as a fuel for these tests was undertaken to simplify the measurements and to maximize the length of the soot-containing region (this is longest for acetylene-fueled flames because other fuel types do not generate soot until they have decomposed to yield acetylene as will be shown by the results to be discussed in the following).

2.3 Experimental Results

Soot Structure. A typical TEM photograph of a soot particle (soot aggregate) collected from the present flames is illustrated in Fig. 2. This soot aggregate was obtained during a space-based experiment with a nonbuoyant soot emitting ethylene-fueled laminar jet diffusion flame in still air at 100 kPa; thus, this soot aggregate is typical but somewhat larger than soot aggregates found in buoyant laminar jet diffusion flames having much shorter residence times. The present soot aggregates consist of nearly monodisperse (at a particular flame condition) spherical primary soot particles that generally have diameters smaller than 60 nm. These primary particles collect into soot aggregates that have rather broad ranges of numbers of primary particles per aggregate (typically having 2-2000 primary particles per aggregate). These aggregates are mass fractal objects having fractal dimensions of roughly 1.8 whose optical properties are reasonably represented by the Rayleigh-Debye-Gans scattering approximation with optical models for these particles generally called Rayleigh-Debye-Gans/Polydisperse-Fractal-Aggregate (RDG/PFA)

Table 4. Nonpremixed Flame Test Conditions[a]

Flame	Fuel	% Fuel in Fuel Stream	Oxidant	% O_2 in Oxidant Stream	Burner Diameter (mm)	Pressure (atm)	Flame Length (mm)
Acetylene-nitrogen/air flames, from Xu and Faeth (2001):							
1	C_2H_2/N_2	16.9	Air	21.0	34.8	1.0	82
2	C_2H_2/N_2	15.1	Air	21.0	34.8	1.0	88
3	C_2H_2/N_2	17.1	Air	21.0	34.8	1.0	103
Hydrocarbon-nitrogen/air flames, from El-Leathy et al. (2003a):							
4	C_2H_4/N_2	100.0	Air	21.0	34.8	1.0	100
5	C_3H_6/N_2	18.8	Air	21.0	34.8	1.0	100
6	C_3H_8/N_2	100.0	Air	21.0	34.8	1.0	100
7	$C_6H_6(4\%)/C_2H_2/N_2$	85.4	Air	21.0	34.8	1.0	90
8	$C_6H_6(11\%)/C_2H_2/N_2$	88.5	Air	21.0	34.8	1.0	90
9	$C_6H_6(29\%)/C_2H_2/N_2$	92.3	Air	21.0	34.8	1.0	90
Acetylene-nitrogen/air flames, from Kim et al. (2003):							
10	C_2H_2/N_2	21.0	Air	21.0	3.3	1.0	50
11	C_2H_2/N_2	39.0	Air	21.0	3.3	0.5	50
12	C_2H_2	100.0	Air	21.0	3.3	0.25	50
13	C_2H_2	100.0	Air	21.0	3.3	0.125	50

[a]Fuel port flowing mixtures vertically upward in coflowing oxidant stream.

[b]Concentrations are percent by volume.

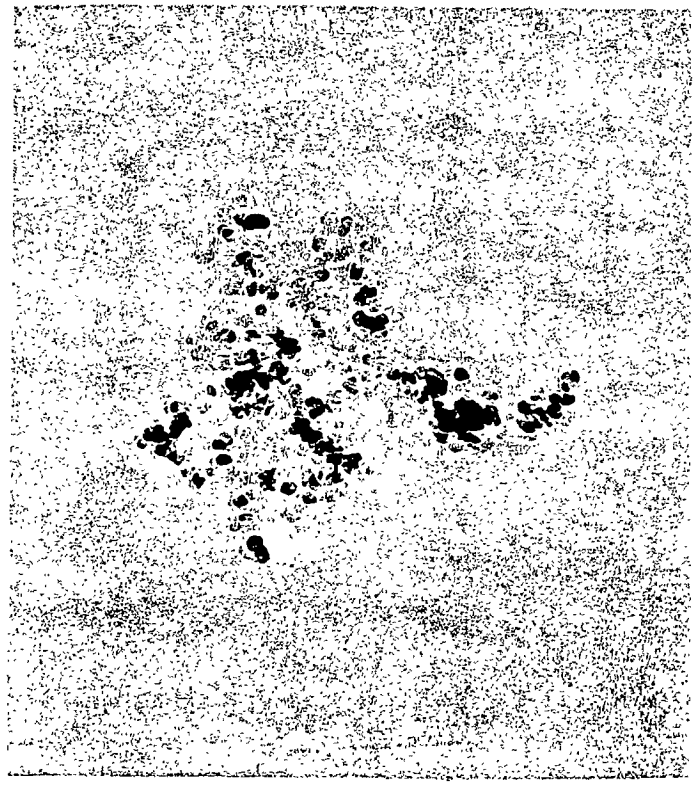

Fig. 2 TEM photograph of a typical soot aggregate in a nonbuoyant round ethylene-fueled laminar jet diffusion flame in still air at 1 atm. This aggregate was in the soot layer beyond the flame tip (z=55 mm) of a soot-emitting flame. The aggregate has a maximum dimension of 1100 nm. From Urban et al. (1998).

theory, see Köylü and Faeth (1992,1993,1994a,b,1996) and Köylü et al. (1995) for more details about the optical and radiative properties of soot aggregates.

Structure of Flames for the Large Diameter Burner. Discussion of the structure of soot-containing flames will begin with the flames observed at atmospheric pressure using the large diameter burner (33.4 mm burner from Xu and Faeth (2003a)). Typical measurements of the structure of the soot-containing region of these flames are illustrated in Figs. 3-5. In particular, the structure of the acetylene-nitrogen/air flame at atmospheric pressure (Flame 2) in Fig. 3 is qualitatively similar to the other acetylene-nitrogen/air flames at atmospheric pressure observed using this burner (Flames 1 and 3); the structure of the ethylene/air flame at atmospheric pressure (Flame 4) in Fig. 4 is typical of the propylene-nitrogen/air and propane/air flames at atmospheric pressure (Flames 5 and 6); and the structure of the acetylene-benzene-nitrogen/air flame (Flame 9) in Fig. 5 is typical of the other acetylene-benzene-nitrogen/air flames at atmospheric pressure (Flames 7 and 8).

Properties along the flame axes are plotted for the three large burner flames in Figs. 3-5. Properties considered include gas (soot) temperatures, streamwise gas velocities, soot volume fractions, primary soot particle diameters, concentrations of major gas species and concentrations of radical (H, OH and O) species. Corresponding residence times, found by integrating the velocity measurements, are indicated at the top of the plots. The residence times are relative to the first positions where detectable soot volume fractions were observed (z=10-20 mm) for the three flames). The stoichiometric (ϕ=1) or flame sheet condition, for the three flames is at z=81-110 mm; this condition is marked on Fig. 4 by a dashed line; for the other flames, the (ϕ=1 condition falls to the left of the region that is plotted. The end of the luminous, or soot-containing, region of the flames in Figs. 3, 4 and 5 are at z=80, 100 and 90 mm, respectively, although soot concentrations near these boundaries were too small to be accurately measured using present methods. Finally, it is convenient to divide the present flames into two regions separated by the location of the maximum soot concentration condition, as follows: (1) the region upstream of this condition where soot formation dominates other soot reaction processes and soot concentrations increase with increasing distance from the burner exit, which will be called the soot formation region, and (2) the region downstream of this condition where soot oxidation dominates other soot reaction processes and soot concentrations decrease with increasing distance from the burner exit, which will be called the soot oxidation region.

Gas (soot) temperatures plotted in Figs. 3-5 reach a broad maximum in the soot formation region, somewhat before the flame sheet is reached. The temperature range of these flames is relatively narrow (1600-1850 K) which is smaller than the adiabatic flame temperatures for these conditions (1900-2370 K) due to radiative heat losses mainly caused by continuum radiation

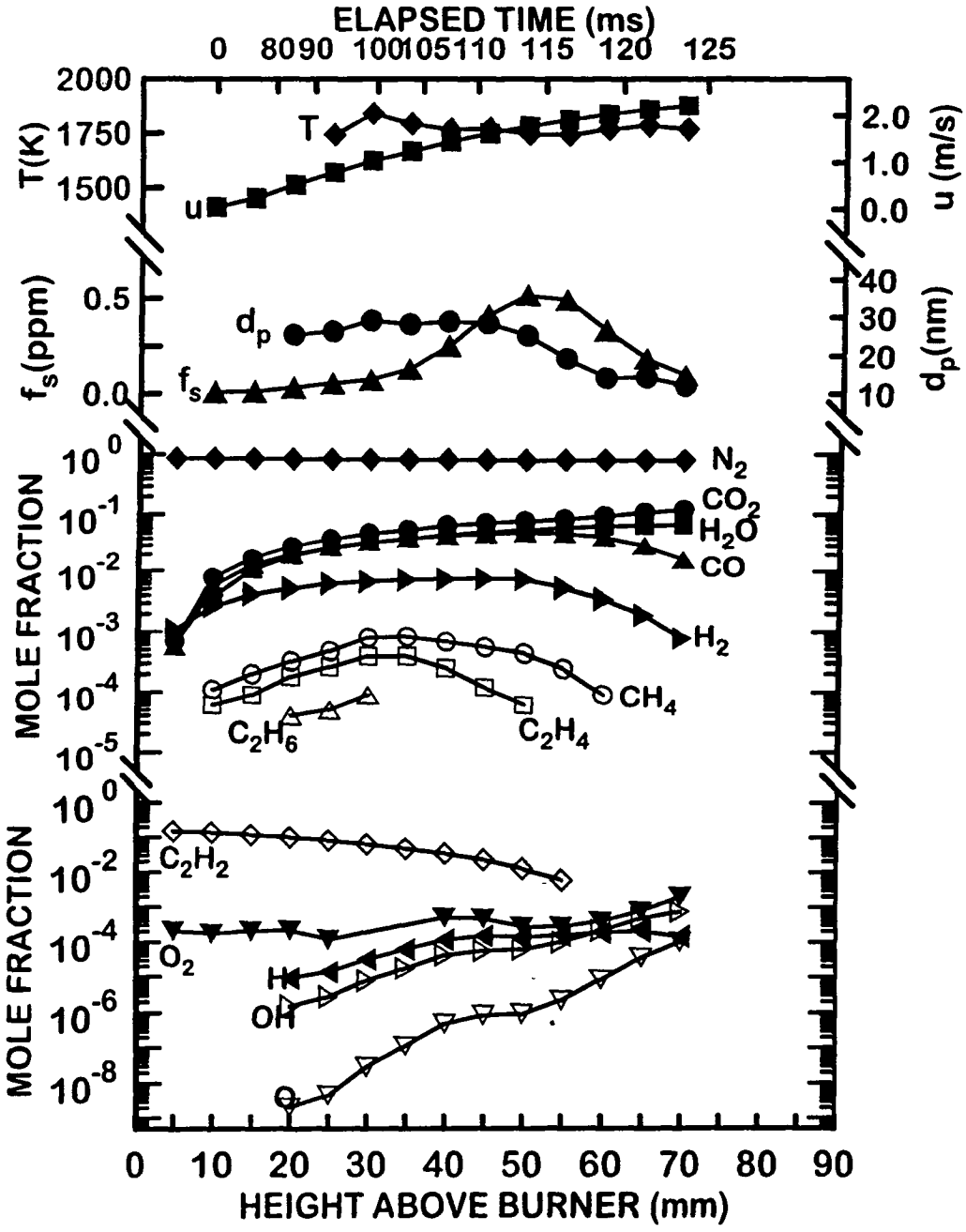

Fig. 3 Measured soot and flame properties of an acetylene-nitrogen-fueled laminar jet diffusion flame burning in coflowing air at atmospheric pressure; Flame 2, fuel stream of 15.1%, C_2H_2 and 84.9% N_2 by volume. From Xu and Faeth (2001).

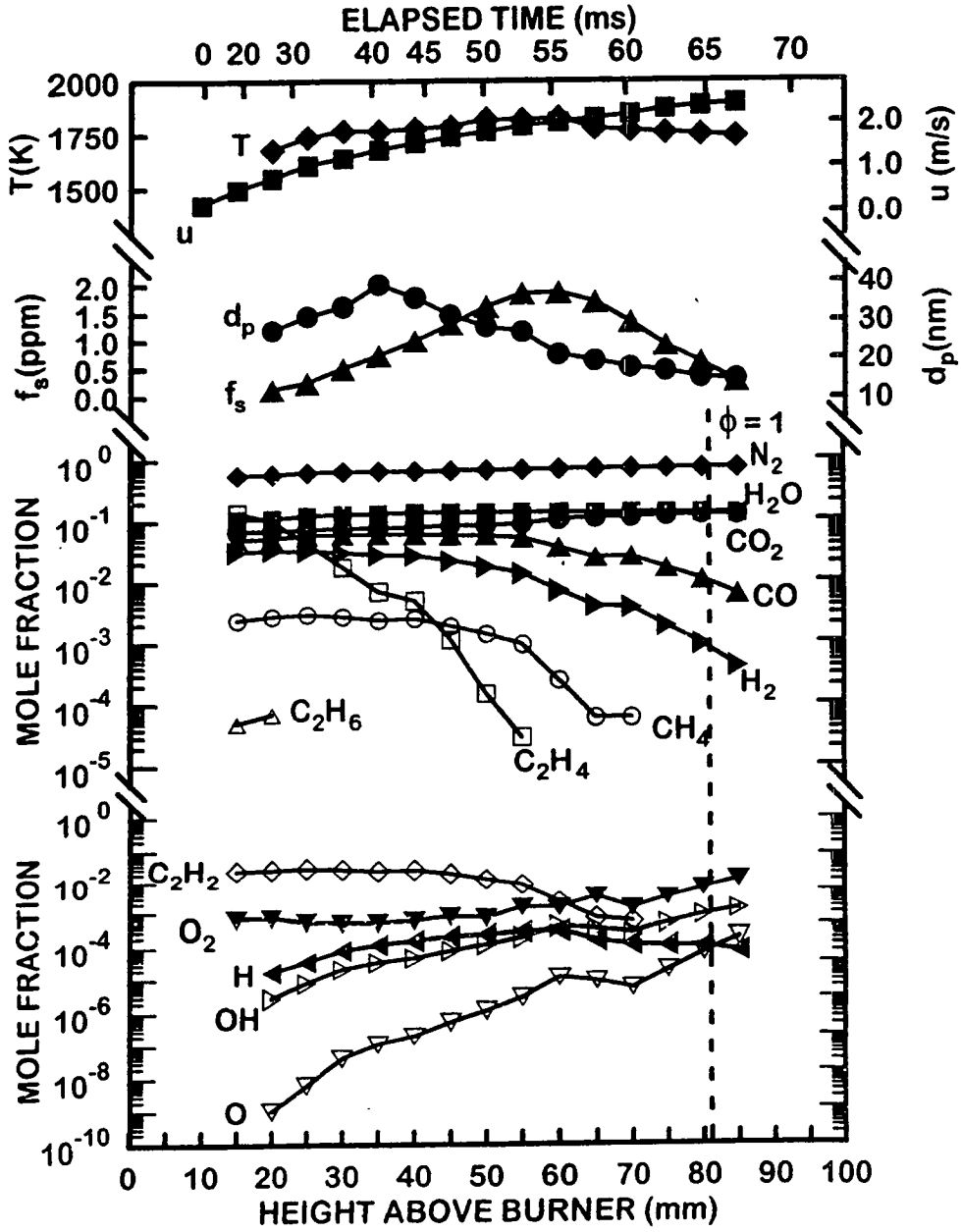

Fig. 4 Measured soot and flame properties of an ethylene-fueled laminar jet diffusion flame burning in coflowing air at atmospheric pressure; Flame 4, fuel stream of 100% C_2H_4 by volume. From El-Leathy et al. (2003a).

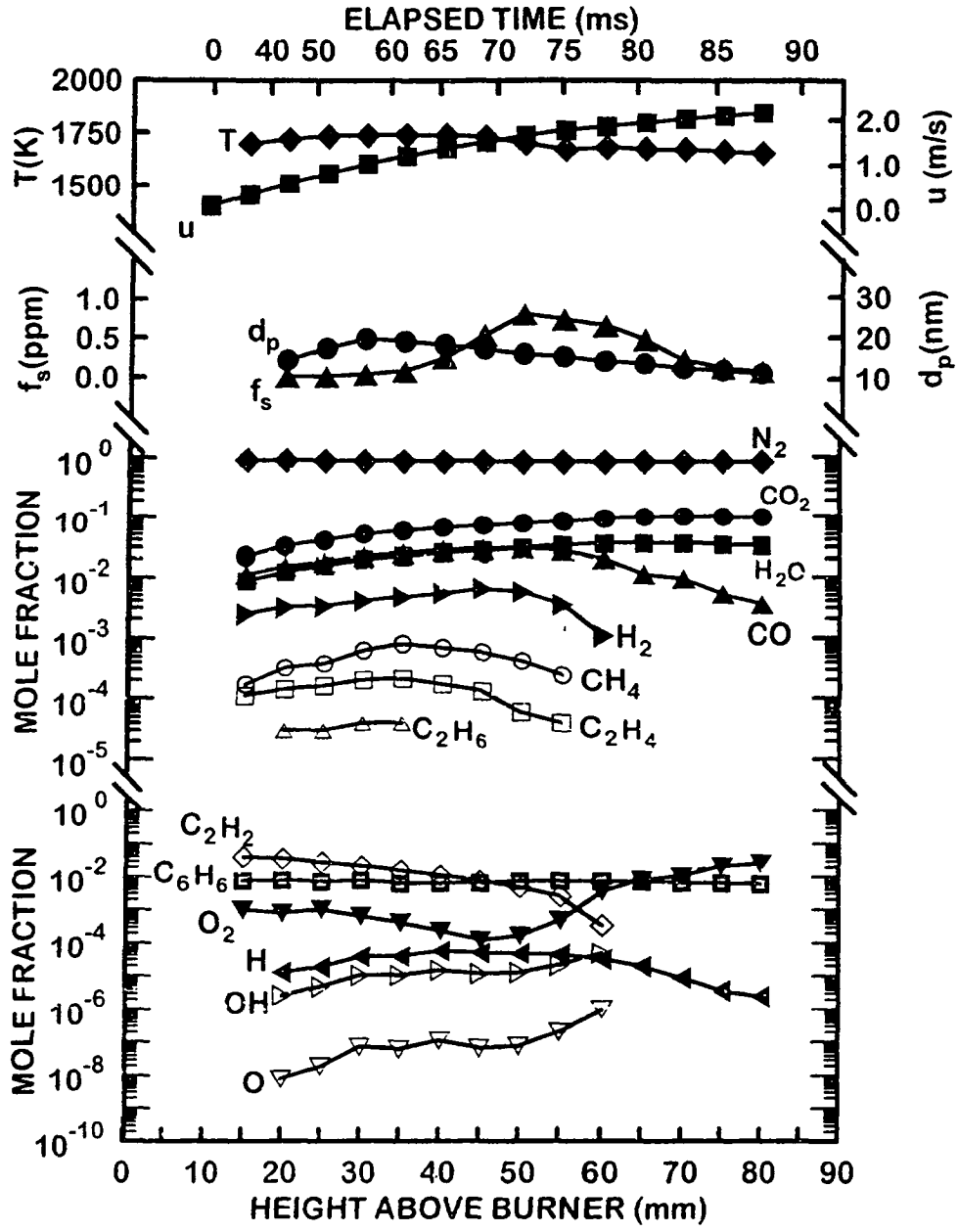

Fig. 5 Measured soot and flame properties of an acetylene-benzene-fueled laminar jet diffusion flame burning in coflowing air at atmospheric pressure; Flame 9, fuel stream of 2.2% C_6H_6, 5.5% C_2H_2 and 92.3% N_2 by volume. From El-Leathy et al. (2003a).

from soot. This behavior is typical of all the diffusion flames that have been studied using the large burner during the present investigation (Flames 1-19).

Gas velocities increase with increasing distance from the burner exit in Figs. 3-5. This behavior comes about due to buoyant acceleration of the flow from the relatively small velocities at the burner exit for flames using the large diameter burner. This velocity variation causes corresponding distortion of the elapsed time scale seen at the top of Figs. 3-5.

Primary soot particle diameters reach maximum values relatively early in the soot formation region in Figs. 3-5. This behavior is caused by accelerating soot primary particle nucleation rates with increasing streamwise distance, which is caused by progressively increasing H concentrations with increasing distance from the burner exit as discussed by Xu and Faeth (2001). This behavior also causes the relatively few primary soot particles formed near the soot inception conditions, that become large due to long periods of soot surface growth in the soot formation region, to be superseded by the much larger number of primary soot particles formed later in the soot formation process that are smaller due to smaller times of soot surface growth.

Significant levels of soot formation (evidenced by finite soot volume fractions) are generally associated with conditions where detectable amounts of H (10 ppm) are first observed. For all the fuels, this condition involved relatively large acetylene concentrations, e.g., concentrations of 4-10% by volume for the conditions illustrated in Figs. 3-5. Soot formation becomes small again when maximum soot concentrations are reached, which occurs in the presence of relatively large concentrations of H (100-200 ppm), when acetylene concentrations become smaller than roughly 1% by volume. An interesting feature of the maximum soot concentration condition where soot formation becomes small when benzene is a portion of the fuel, e.g., Fig. 5, is that this event definitely is correlated with conditions where the concentrations of acetylene become small, whereas, the concentrations of benzene remain relatively constant in this region before finally disappearing near the flame sheet (see the region near the maximum soot concentration condition in Fig. 5). In addition, benzene was only observed with detectable concentrations in the benzene-fueled flames.

The concentrations of major gas species in Figs. 3-5 are similar to observations in other soot-containing laminar diffusion flames that have been studied, for example, Sunderland et al. (1995,1996) and Lin et al. (1996). When acetylene is the fuel, e.g., in Fig. 3, its concentration progressively decreases with increasing distance from the burner exit. For fuels other than acetylene, e.g., Figs. 4 and 5, however, the original fuel generally disappears relatively close to the burner exit to yield hydrogen and hydrocarbon species that are relatively robust in high-temperature flame environments, particularly acetylene which is relatively stable at high

temperatures. Acetylene is especially important as a fuel decomposition product because it is thought to be the major building block of both PAH, which leads to soot nucleation, and soot surface growth, see Howard (1990), Colket and Hall (1994), Frenklach and Wang (1994,1999) and Kazakov et al. (1995). Benzene as a fuel is an apparent exception to this behavior in Fig. 5, but even benzene largely disappears near the burner exit, leaving a relatively small but nearly constant benzene concentration in the soot-containing region with benzene only finally disappearing near the flame sheet. In addition, concentration distributions of flames fueled with hydrocarbons other than acetylene are qualitatively similar to concentration distributions of acetylene within flames fueled with acetylene. The final combustion products, CO_2 and H_2O, increase with increasing streamwise distance throughout the soot formation region in Figs. 3-5, reaching broad maxima near the flame sheet (the ϕ=1 condition). Intermediate combustion products associated with water-gas equilibrium, CO and H_2, are present at relatively large concentrations throughout the soot formation region, reaching broad maxima somewhat upstream of the flame sheet. Finally, nitrogen concentrations remain relatively uniform in the regions of the flames burning in air that are illustrated in Figs. 3-5, because nitrogen concentrations dominate all conditions near and beyond the flame sheet due to the large concentration (79% by volume) of nitrogen in air.

Concentrations of O_2 in Figs. 3-5 either progressively increase with increasing distance from the burner exit (Figs. 3 and 4) or progressively increase as the flame sheet is approached after reaching a broad minimum near the burner exit (Fig. 5). The former behavior follows because O_2 concentrations at the flame sheet are relatively large. The latter behavior probably is caused by some leakage of coflowing O_2 into the fuel-rich region of the flames through the gap between the burner exit and the point where the flames are attached. Thus, O_2 is invariably present at concentrations on the order of 0.1% (by volume) throughout most of the soot formation region of the present flames. In addition, concentrations of fuel-like species, particularly H_2 and CO, penetrate well into the fuel-lean region. Thus, the present flames generally do not satisfy approximations made during simplified classical analysis of laminar diffusion flames in that there is considerable overlap of fuel-like and oxidant-like species in the region of the flame sheet.

In Figs. 3-5, concentrations of OH and O increase monotonically as the flame sheet is approached, whereas concentrations of H reach a broad maximum within the soot formation region before decreasing somewhat as the flame sheet is approached. For near-atmospheric pressure conditions, H and OH exhibit superequilibrium concentrations throughout the soot-containing region, particularly as the flame sheet is approached. Finally, species that past measurements in diffusion flames have shown to be responsible for soot surface growth (C_2H_2 and H) from Xu and Faeth (2001), and for soot surface oxidation (O_2 and OH) from Xu et al. (2003) are seen to be present within the soot formation region; therefore, soot surface growth and

oxidation proceed at the same time in the soot formation regions of the flames illustrated in Figs. 3-5, as well as in all other diffusion flames studied thus far (Flames 1-13).

Structure of Flames for the Small-Diameter Burner. Typical measurements of the structure of the soot-containing region of the flame for the small-diameter burner are illustrated in Figs. 6 and 7. These measurements were limited to acetylene-fueled flames because study of various fuels for soot-containing diffusion flames by El-Leathy et al. (2003a) showed that although fuel type modified temperatures and species concentrations in these flames, it had a negligible effect on fundamental soot surface growth and oxidation properties. In particular, the acetylene-nitrogen/air flame at atmospheric pressure (Flame 10) in Fig. 6 is designed to illustrate effects of increased burner exit velocities by comparison with a similar flame (Flame 2) on the large-diameter burner illustrated in Fig. 3. Furthermore, the acetylene/air flame at 0.125 bar (Flame 13), illustrated in Fig. 7 is designed to illustrate effects of pressure by comparison to a similar flame (Flame 10) at atmospheric pressure in Fig. 6. Properties are plotted in Figs. 6 and 7 in the same manner as for the large diameter burners in Figs. 3-5. In the case of small diameter flames, however, the stoichiometric condition appears within the region that is plotted, whereas luminous flame lengths are all at z=50 mm and are near the right-hand boundaries of the figures. As before, soot concentrations near the luminous flame boundaries were too small to be measured accurately, although the yellow luminosity from continuum radiation for soot was still visible.

Gas (soot) temperatures along the flame axes in Figs. 6 and 7 reach a maximum well before the flame sheet is reached. This behavior is similar to all other diffusion flames studied in this laboratory (Flames 1-13) and is caused by continuum radiation heat losses from soot.

The burner used for the flames illustrated in Figs 6 and 7 has a diameter roughly ten times smaller than that for the flames illustrated in Figs. 3-5 whereas fuel stream mass flow rates for all the flames were not very different. As a result, the burner velocities at the exit of the small diameter burners are relatively large (2.5-12 m/s) compared to the large diameter burners (roughly 0.01 m/s). As a result, the small burner flames are only weakly buoyant and flow velocities within them decrease with increasing distance from the burner exit, similar to nonbuoyant flames.

Similar to the earlier observations of soot-containing diffusion flames discussed in connection with Figs. 3-5, primary soot particle diameters in Figs. 6 and 7 reach maximum values relatively early in the soot formation region. Similarly, significant levels of soot formation were associated with the first streamwise locations where detectable concentrations of H were observed, because acetylene, the other reactant of the HACA soot surface growth mechanism, was always present near the burner exit for the present acetylene-fueled flames.

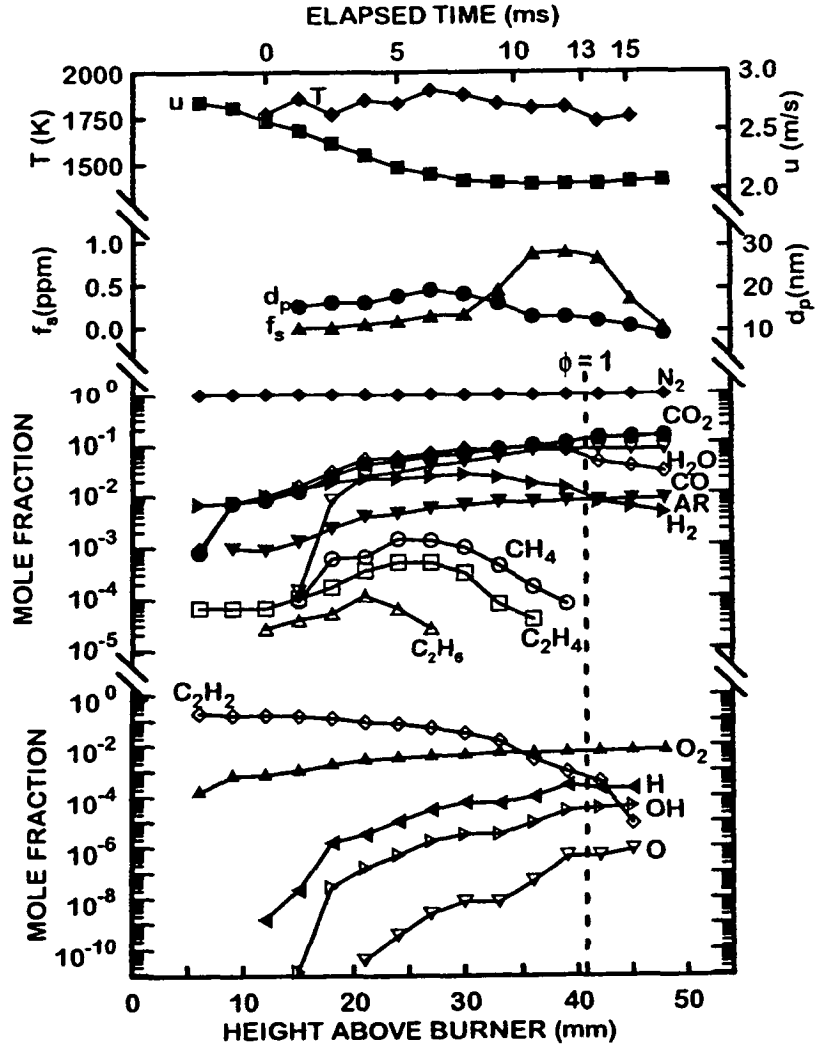

Fig. 6 Measured soot and flame properties of an acetylene-nitrogen-fueled laminar jet diffusion flame burning in coflowing air at atmospheric pressure; Flame 10, fuel stream of 21.0% C_2H_2, and 79.0% N_2 by volume. From Kim et al. (2003).

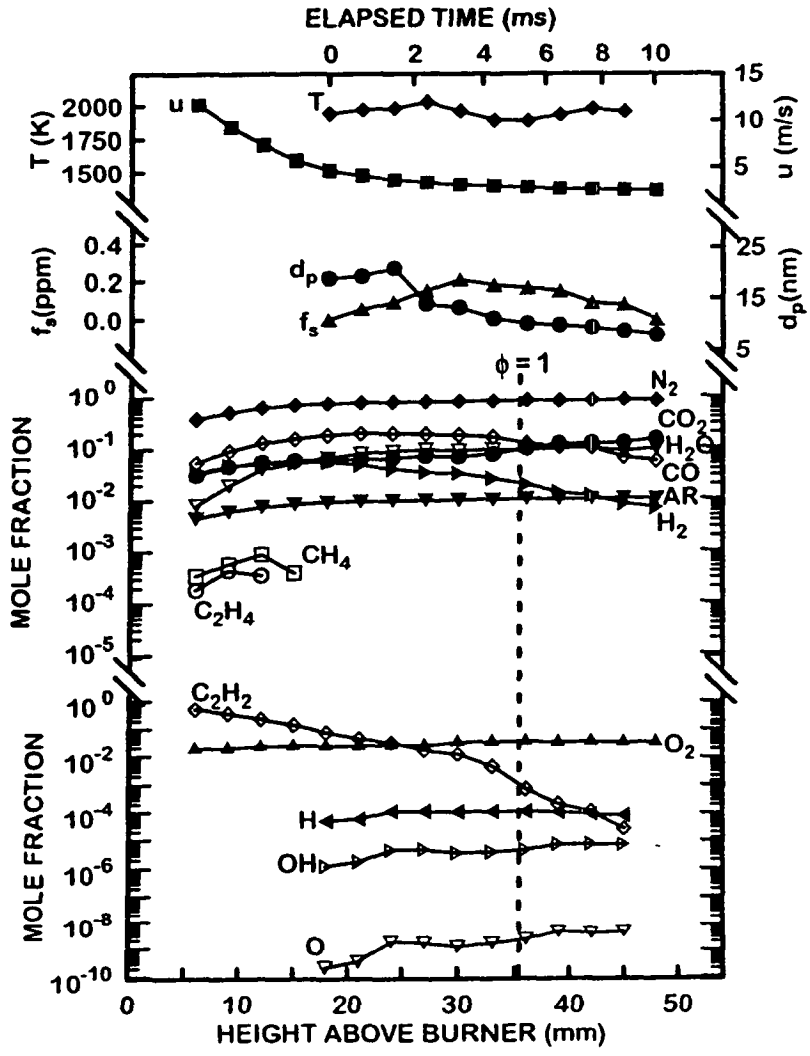

Fig. 7 Measured soot and flame properties of an acetylene-fueled laminar jet diffusion flame burning in coflowing air at a pressure of 0.125 atm; Flame 13, fuel stream of 100% C_2H_2. From Kim et al. (2003).

Soot formation again became small at the maximum soot concentration condition in the presence of large concentrations of H but where acetylene concentrations become smaller than 0.1% by volume. This behavior is also similar to the behavior of the diffusion flames discussed in connection with Figs. 3-5. Finally, concentrations of major stable gas species in the small burner flames were generally similar to the behavior of the large burner flames discussed in connection with Figs. 3-5.

In general, concentrations of O and OH increase as the flame sheet is approached whereas H tends to reach a broad maximum near or somewhat before the flame sheet is reached. Maximum concentrations of H in all the flames are surprisingly nearly the same at 0.01 percent by volume with maximum OH concentrations near or beyond the flame sheet having a similar magnitude. Maximum concentrations of O are significantly smaller and more variable, reaching values of 0.000001-0.01 percent by volume. An interesting effect of pressure on the flames can be seen by comparing Figs. 6 and 7 for acetylene-fueled flames at 1.0 and 0.1 atm. It is seen that radical concentrations in low-pressure flames are nearly constant compared to significant increases of radical concentrations as the flame sheet is approached for the atmospheric pressure flames.

Similar to the flames on the large burner, concentrations of species potentially responsible for soot oxidation, e.g., O_2, CO_2, H_2O, O and OH, are all present in the soot formation regions of the flames. Thus, soot surface growth and oxidation proceed at the same time in the low pressure flames, similar to the flames at atmospheric pressure.

2.4 Conclusions

Flame structure was studied for coflowing buoyant laminar jet diffusion flames involving the test conditions summarized in Table 4: acetylene, ethylene, propylene, propane and benzene as fuels all burning in air; pressures of 0.1-1.0 atm, burner diameters of 3.3 and 34.8 mm, and visible flame lengths of 50-103 mm with the reactants at normal temperature. Major conclusions of the study are as follows:

1. In all flames considered thus far (except naturally for acetylene and ethylene-fueled flames), the original fuel largely decomposes near the burner exit, yielding species that generally are associated with soot surface growth, e.g., CH_4, C_2H_2, C_2H_4, H_2 and H, among others. The yields of these species are affected by the fuel type but it will be shown later that soot surface reaction rates generally are independent of fuel type.

2. Laminar diffusion flames at subatmospheric pressures were qualitatively similar to those at atmospheric pressure. The main difference was that low pressure flames tend to have relatively uniform concentrations of radicals (H, OH and O) over the soot-containing region whereas concentrations of these radicals tend to increase as the flame sheet is approached for the atmospheric pressure flames.

3. The region of soot formation in the present diffusion flames had significant concentrations of species potentially associated with soot oxidation, e.g., O_2, CO_2, H_2O, O and OH; therefore, soot formation, including soot surface growth, must be occurring at the same time as soot surface oxidation.

4. The measurements showed that significant degrees of soot formation begin near the burner exit once H first appears in a prevailing condition where acetylene concentrations are relatively large and that soot formation ends near the flame sheet where acetylene disappears in a prevailing condition where H concentrations are relatively large. This behavior is consistent with soot surface growth being dominated by Hydrogen-Abstraction/Carbon-Addition (HACA) mechanisms typified by Colket and Hall (1994), Frenklach and Wang (1990,1994) and Kazakov et al. (1995). Finally, measurable concentrations of benzene were only observed for benzene-fueled flames; even in this case, however, benzene concentrations in the soot-containing region were nearly constant, were relatively small (less than 1% by volume), and were not particularly correlated with either the onset or the end of soot formation.

3. Soot Surface Reaction Properties

3.1 Introduction

Present and past measurements of laminar premixed and diffusion flames were used to study soot surface growth and oxidation. Major assumptions used when obtaining soot surface growth and oxidation rates from the flame structure measurements were as follows: soot surface growth, rather than soot nucleation, dominates soot mass production; soot surface oxidation dominates surface oxidation (limiting soot mass degrees of oxidation to less than 70% in order to avoid problems of the development of soot surface porosity and internal oxidation observed by Neoh et al. (1984) at larger degrees of soot oxidation); effects of diffusion (Brownian motion) and thermophoresis on soot motion are small, so that soot particles convect along the axes of the flames at the local gas velocity; soot density is a constant, taken to be 1850 kg/m^3 from Köylü et al. (1995); and the surface area available for soot surface growth and oxidation is equivalent to constant diameter spherical primary soot particles that meet at a point, see Sunderland et al.

(1995,1996), Lin et al. (1996), Xu et al. (1997,1998,2003) and El-Leathy et al. (2003a) for justification of these assumptions.

The first soot formation and oxidation property of importance is the number of primary soot particles per unit volume, found from the measured soot volume fractions and primary soot particle diameters, as follows (Sunderland et al., 1995):

$$n_p = 6f_s/(\pi d_p^3) \quad (1)$$

The experimental uncertainties (95% confidence) of n_p are estimated to be less than 32% for $f_s \geq$ 0.1 ppm, increasing inversely proportional to f_s for smaller values of f_s. The soot surface area per unit volume is given by the same measurements, as follows(Sunderland et al. 1995):

$$S = 6f_s/d_p \quad (2)$$

The experimental uncertainties (95% confidence) of S are estimated to be less than 16% for $f_s \geq$ 0.1 ppm, increasing inversely proportional to f_s for smaller values of f_s. Defining the soot surface growth rate as the rate of increase of soot mass per unit surface area and time, and the soot surface oxidation rate as the rate of decrease of soot mass per unit surface area and time, conservation of soot mass along streamlines at the axes of the flames, under the previous assumptions, gives the soot surface growth and oxidation rates, as follows (Sunderland et al., 1995):

$$w_g = - w_{ox} = (\rho/S)d(\rho_s f_s/\rho)/dt \quad (3)$$

where present measurements of species concentrations and temperatures yield the gas density, assuming an ideal gas mixture, and the minus sign is inserted so that w_{ox} is a positive number. The temporal derivative in Eq. (3) was found from three-point least square fits of the argument; similar to past work, see (Sunderland et al. 1995). Finally, as noted earlier, consideration of soot surface oxidation was limited to early soot oxidation (soot mass consumption less than 70%) where problems of soot primary particle porosity and internal oxidation of primary soot particles do not yet occur, see Neoh et al. (1984). Estimated experimental uncertainties (95% confidence) of soot surface growth rates are less than 30%; estimated experimental uncertainties of soot surface oxidation rates are comparable.

3.2 Soot Surface Growth Rates

Determination of experimental soot surface growth rates, and use of these results to evaluate existing soot surface growth rate mechanisms, was limited to the atmospheric pressure premixed flames summarized in Table 3 (premixed Flames 1-10) and the atmospheric pressure diffusion flames summarized in Table 4 (diffusion Flames 1-9). Gross soot surface growth rates for these premixed and diffusion flames were corrected for effects of soot surface oxidation because soot surface growth and oxidation proceed at the same time as noted in connection with Figs. 3-7. The correction for soot surface oxidation was made using the results of Xu et al. (2003) concerning soot oxidation in laminar premixed and diffusion flames; this work will be discussed in Section 2 of this report. Thus, it was assumed that soot surface oxidation was dominated by the OH oxidation mechanism, after allowing for direct soot surface oxidation by O_2 based on the experimental correlation of Nagle and Strickland-Constable (1962). This procedure was appropriate because soot surface oxidation throughout the soot surface growth region involves fuel-rich conditions that are known to be dominated by the OH soot surface oxidation mechanism, see the discussion of this observation due to Neoh et al. (1980). It was found that effects of the correction for soot surface growth rates for soot surface oxidation was small, except when soot surface growth rates themselves became small toward the end of the soot formation region. Thus, in order to be conservative about potential effects of soot surface oxidation, determination of soot surface growth rates, corrected for effects of soot surface oxidation, were limited to conditions where estimated soot surface oxidation rates never exceeded half the gross soot surface growth rate, similar to past work, see Xu and Faeth (2001) and references cited therein.

Soot surface growth rates were interpreted using the HACA soot surface growth mechanisms of Colket and Hall (1994), and Frenklach and coworkers (Frenklach and Wang 1990,1994; Kazakov et al., 1995), in order to maintain consistency with past evaluations of these mechanisms and due to the past success of these mechanisms for correlating soot surface growth rates in premixed ethylene/air and methane/oxygen flames (Xu et al., 1997,1998). In all cases, soot surface growth rates corrected for soot surface oxidation (called net soot surface growth rates in the following) were expressed as follows:

$$w_g = \alpha_i R_i \tag{4}$$

where i=CH or FW denotes reaction parameters for the HACA soot surface growth rate mechanisms of Colket and Hall (1994) and Frenklach and coworkers (1990,1994,1995), which were found from the measurements. The details of these mechanisms, the formulas for the R_i, and the reaction-rate parameters for the R_i, can be found in Xu et al. (1997). The parameters, α_i,

are empirical steric factors having values on the order of unity: α_{CH} is specified to be a constant (Colket and Hall, 1994) whereas α_{FW} is specified to be a function of temperature that has a negative activation energy, i.e., α_{FW} tends to decrease as the temperature of the soot-containing gas mixture increases (Frenklach and Wang, 1990,1994; Kazakov et al., 1995),

As a first approximation for all of the premixed and diffusion flames considered during the present investigation, the R_i are proportional to the product $[H][C_2H_2]$. Thus, values of $w_g/[C_2H_2]$ measured for premixed ethylene/air flames by Xu et al., (1997), premixed methane/oxygen flames by Xu et al., (1998), nonpremixed acetylene-nitrogen/air flames by Xu and Faeth (2001) and nonpremixed hydrocarbon-nitrogen/air flames by El-Leathy et al. (2003a) (after correcting all the measurements for effects of soot surface oxidation using the OH and O_2 approach based on the measurements of Xu et al. (2003a)), are plotted as a function of [H] in Fig. 8 in order to provide a direct test of the main features of the HACA soot surface growth rate mechanisms without the intrusion of uncertainties due to the numerous empirical parameters in the original detailed mechanisms. The results for premixed and nonpremixed (diffusion) flames in Fig. 8 are distinguished by denoting them by open and closed symbols, respectively. Finally, an empirical correlation of the measurements is also illustrated in Fig. 8, obtained as an average for all the flames.

First of all, it should be noted that present estimates of soot surface growth rates (correlated for effects of soot surface oxidation) were baselined using earlier approximate methods of correcting for soot surface oxidation rates that considered soot surface oxidation by CO_2, H_2O and O_2 rather than by OH and O_2, e.g., the soot surface growth measurements of Sunderland et al. (1995), Sunderland and Faeth (1996), Lin et al. (1996), Xu et al. (1997,1998) and Xu and Faeth (2001). In both the present and earlier work, a conservative approach was taken where only soot surface growth conditions where the correction for soot surface oxidation was less than half the gross soot surface growth rate were considered, this limitation caused the correction for soot surface oxidation to largely indicate conditions where the correction for soot surface oxidation was becoming appreciable so that these conditions could be excluded during the evaluation of the HACA soot surface growth mechanisms. As a result of this conservative approach, however, the earlier and present estimates of net soot surface growth rates were essentially the same.

Considering the present net soot surface growth rates in Fig. 8, there is a tendency for $w_g/[C_2H_2]$ to be slightly larger for the diffusion flames than for the premixed flames, at a given value of [H], when plotted to highlight the leading term of the HACA soot surface growth rate expressions. This bias, however, is largely due to approximating the entire HACA soot surface growth mechanism by the leading term product $[C_2H_2][H]$, because differences between the

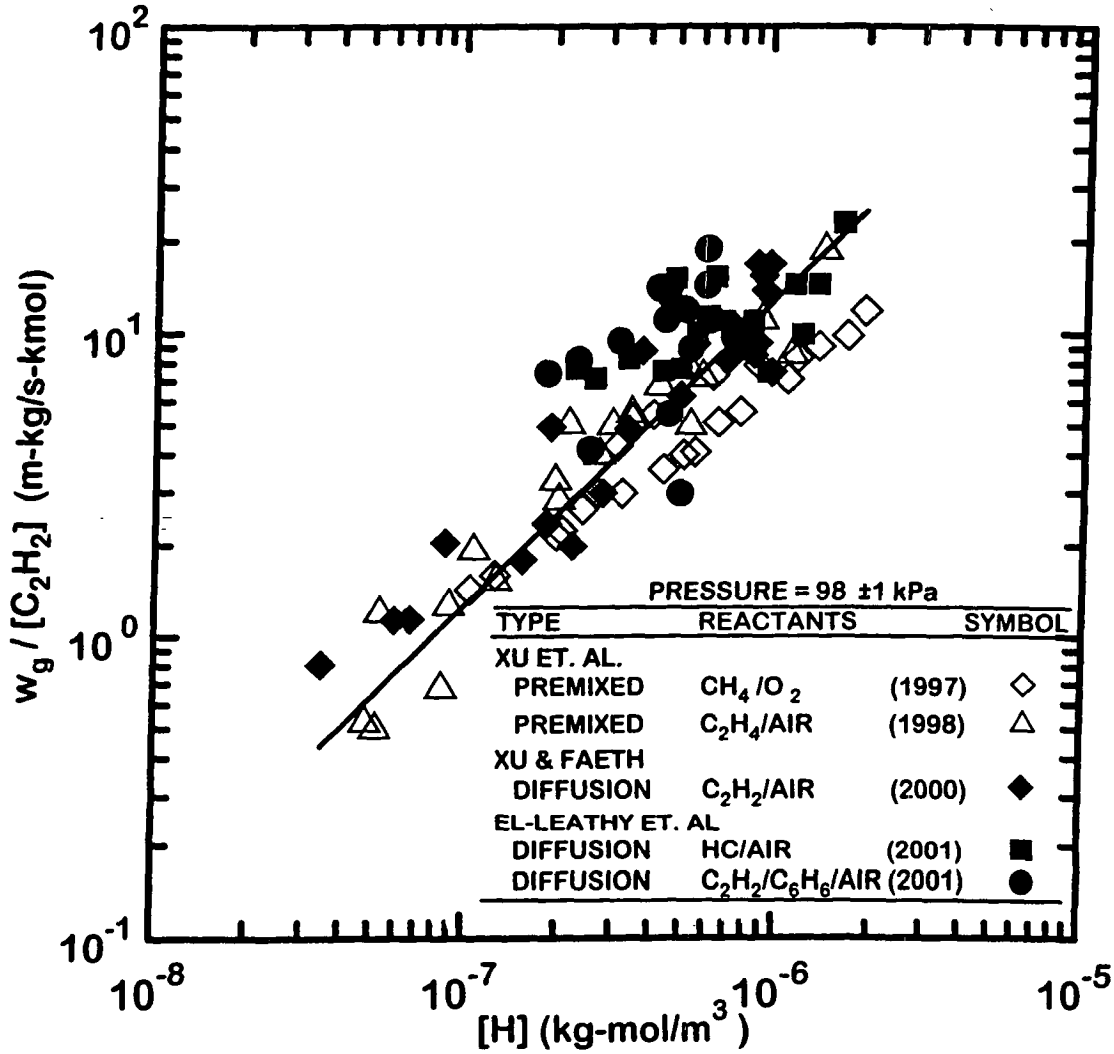

Fig. 8 Soot surface growth rates (corrected for soot surface oxidation) as a function of acetylene and H concentrations for laminar flames at atmospheric pressure. From El-Leathy et al. (2003a).

properties of the soot-containing regions of premixed and diffusion flames affect the higher-order reaction rate terms of the HACA mechanisms. For example, the near-equilibrium and superequilibrium radical concentrations of H in premixed and diffusion flames, affects this correlation significantly. It will be seen subsequently that no distinction between premixed and diffusion flames is observed when the complete HACA mechanisms are considered. Nevertheless, correlation of the net soot surface growth rate results according to the crude $[C_2H_2][H]$ approximation is surprisingly good, and soot surface growth rate properties in premixed and diffusion flames are reasonably consistent with each other in spite of the fundamental differences between their soot formation environments that can be seen by comparing the measured structures of the soot containing regions of premixed flames (Xu et al., 1997,1998), with those in diffusion flames seen in Figs. 3-5 and in Xu and Faeth (2001). In addition, the strong effect of [H] on w_g, evident from the results illustrated in Fig. 8, combined with the near-equilibrium and strongly superequilibrium behavior of H concentrations in the premixed and diffusion flames considered in Fig. 8, respectively, are responsible for the rather poor correlations and enhanced apparent soot surface growth rates of diffusion flames compared to premixed flames, when attempts are made to correlate soot surface growth rates in terms of acetylene concentrations and temperatures alone (Sunderland et al., 1995). Finally, the results in Fig. 3 for premixed and diffusion flames involving a variety of fuel types, clearly indicate that fuel type does not affect the local soot surface growth rates according to the HACA mechanisms. It should be particularly noted that this is still the case for benzene-fueled flames, which might be expected to enhance mechanisms of soot surface growth by involving PAH soot surface growth mechanisms in parallel to the HACA soot surface growth mechanisms. Naturally, this behavior is also consistent with the flame structure results discussed in connection with Figs. 3-7, where particular fuels other than acetylene decompose near the burner exit to yield acetylene concentrations very similar to those encountered in acetylene-fueled flames.

A more direct evaluation of the HACA soot surface growth rate mechanisms is obtained by plotting w_g directly as a function of R_{CH} for the Colket and Hall (1994) mechanism. This type of plot is illustrated in Fig. 9. Results illustrated in Fig. 9 involve premixed flames at atmospheric pressure (Flames 1-9 of Table 3) and diffusion flames at atmospheric pressure (Flames 1-9 of Table 4). All these measurements have been corrected for effects of soot surface oxidation based on the OH and O_2 mechanism as discussed in connection with Fig. 8. Finally, a best-fit correlation of the results for all the flames is also shown on the plot. The corresponding constant steric factor for the Colket and Hall (1994) mechanism based on this fit, is 1.0 with an experimental uncertainty (95% confidence) of $\pm$ 0.2.

Considering the results illustrated in Fig. 9, it is encouraging that the steric factor is on the order of unity, as expected (Colket and Hall, 1994). It is also evident that using the Colket and Hall (1994) mechanism improves the correlation of soot surface growth rates in Fig. 9,

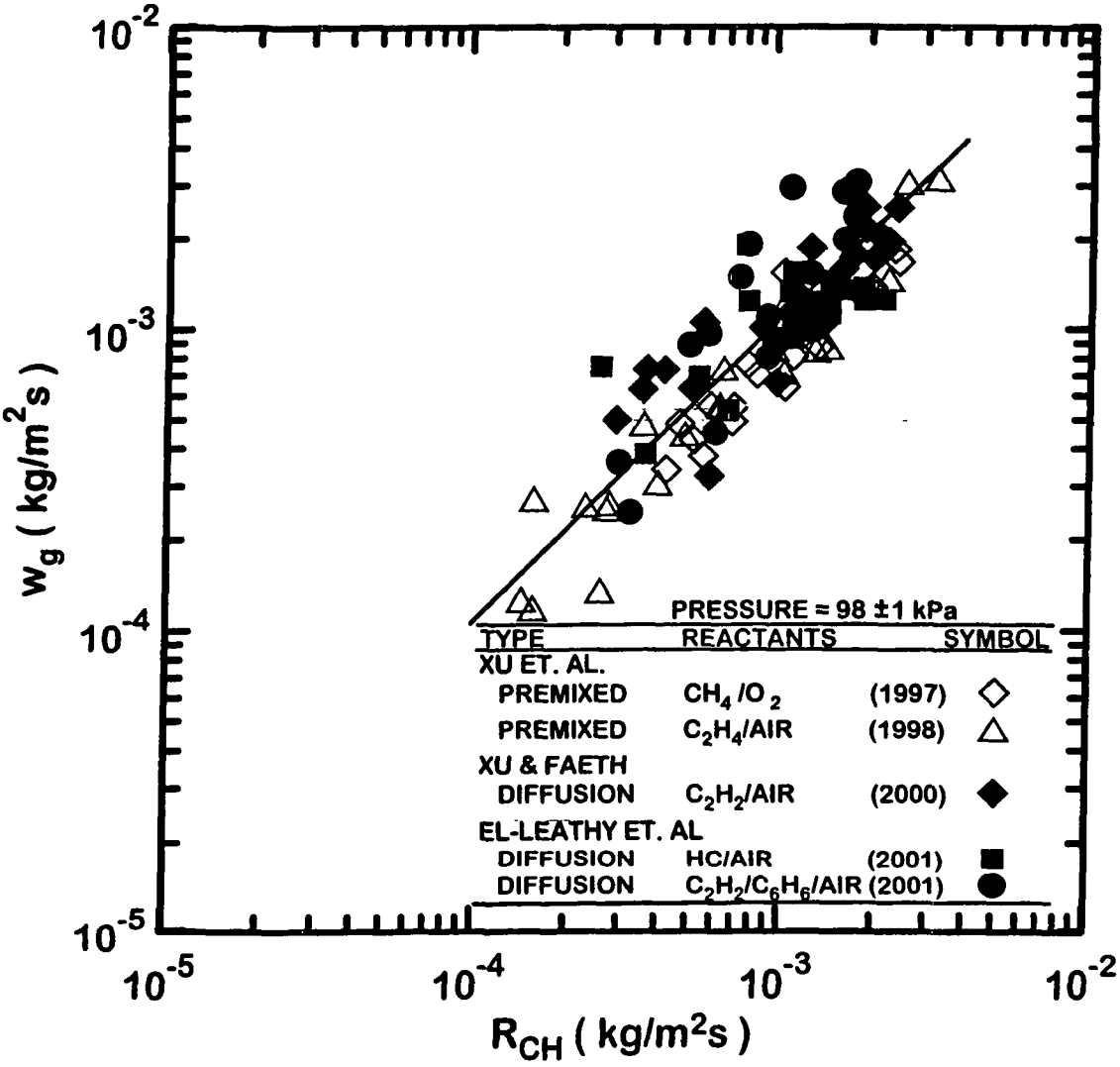

Fig. 9 Soot surface growth rates (corrected for soot surface oxidation) in terms of the HACA mechanism of Colket and Hall (1994) for laminar flames at atmospheric pressure. From El-Leathy et al. (2003a).

compared to the approximate correlation based on only the leading terms of the HACA mechanism illustrated in Fig. 8. In addition, correlation of the soot surface growth rate results for premixed and diffusion flames using the Colket and Hall (1994) mechanism is essentially the same, i.e., there is no statistical significance for the differences between the steric factors found separately for the measurements of premixed and diffusion flames, there clearly is no difference between estimates of w_g based on the HACA mechanism of Colket and Hall (1994) as the hydrocarbon fuel type is varied among the alkyne, alkene, alkane and aromatic fuels considered during the present investigation, i.e., there is no statistical significance to the differences between the values of the steric factors formed for the various hydrocarbon fuels in premixed and diffusion flames that were considered during the measurements illustrated in Fig. 9.

The correlation of α_{FW} for soot surface growth for the complete database of laminar premixed and diffusion flames (corrected for soot surface oxidation similar to the results shown in Figs. 8 and 9) was essentially the same as the results presented for the acetylene-nitrogen/air diffusion flame study of Xu and Faeth (2001), which considered all the premixed flames at atmospheric pressure listed in Table 3 (Flames 1-9) but was limited to the acetylene-nitrogen/air diffusion flames on the large burner listed in Table 4 (Flames 1-3). A complete plot of these results can be found in El-Leathy et al. (2002). The correlation of all the soot surface growth rate data considered here, assuming that $\alpha_{FW}(T)$ could be represented by an Arhennius function, similar to that developed by Xu and Faeth (2001), yielded

$$\alpha_{FW}(T) = 0.0017 \exp(12100/T) \tag{5}$$

where T(K) in this expression. The subsequent plot of w_g as a function of $\alpha_{FW}R_{FW}$ was qualitatively similar to the plot appearing in Xu and Faeth (2001), These results indicated that correlations of measurements of soot surface growth rates in laminar premixed and diffusion flames were essentially the same, that effects of fuel type for laminar premixed and diffusion flames were small, that values of α_{FW} were on the order of unity as expected, and that the negative activation energy implied by the argument of the exponential factor of Eq. (5) corresponds to behavior expected by Frenklach and Wang (1990,1994) and Kazakov et al. (1995) for their HACA soot surface growth rate mechanism.

Similar to earlier findings for HACA soot surface growth rates (Xu et al., 1997,1998; Xu and Faeth, 2001), the HACA soot surface growth rate mechanisms of Colket and Hall (1994), and Frenklach and Wang (1990,1994) and Kazakov et al. (1995), continue to be encouraging, and they may eventually provide the basis for reliable methods to estimate soot surface growth rates in flame environments fueled with hydrocarbons. Uncertainties remain, however, about effects of pressure other than at atmospheric pressure, about effects of temperature greater than

the range considered thus far (1850 K), and about effects of PAH as fuels, on soot surface growth rates in premixed and diffusion flames.

3.3 Soot Surface Oxidation Rates

The present measurements of diffusion flame properties at atmospheric pressure for various fuels burning in air (Flames 1-9 in Table 4) were used to study soot surface oxidation, i.e., early soot oxidation prior to total soot oxidation amounts of 70%, where effects of primary soot particle surface porosity and internal oxidation of primary soot particles are small (Neoh et al., 1984). The assumptions and the formulation used to find soot surface oxidation rates have already been described in Section 3.1 in connection with consideration of soot surface growth rates and will not be repeated here.

Present measurements of soot surface oxidation rates were corrected for effects of soot surface growth rates based on the Hydrogen-Abstraction/Carbon-Addition (HACA) growth rate mechanism of Colket and Hall (1994). In particular, this soot surface growth rate mechanism has provided successful correlations of measured soot surface growth rates in premixed and diffusion flames, see Section 3.2 of this report as well as El-Leathy et al. (2003a) and references cited therein. No condition is considered in the following, however, where the correction for effects of soot surface growth on rates of soot surface oxidation was more than half the gross soot surface oxidation rate in order to minimize effects of current uncertainties about soot surface growth rates on the present measurements of soot surface oxidation rates.

Similar to Neoh et al. (1980,1984), present soot surface oxidation rates, corrected for effects of soot surface growth rates, were converted to collision efficiencies (or reaction probabilities) based on kinetic theory estimates of the collision rates of a given species with the surfaces of primary soot particles. Thus, the collision efficiency, η_i, for a potential oxidizing species, i, is given by the following expression (Sunderland and Faeth, 1996):

$$\eta_i = 4w_{ox}/(C_i[i]\,\bar{v}_i) \tag{6}$$

where C_i is the mass of carbon removed from the surface of the primary soot particles per mole of species i reacting at the surface, [i] is the gas-phase concentrations of i adjacent to the surface, and

$$\bar{v}_i = (8R_uT/(\pi M_i))^{1/2} \tag{7}$$

is the (Boltzmann) equilibrium mean molecular velocity of species i. In the following, values of the η_i will be considered for potential soot surface oxidation by O_2, CO_2, H_2O, O and OH, in turn.

Similar to past studies of soot surface oxidation due to Neoh et al. (1980,1984), Garo et al. (1986,1990) and Haudiquert et al. (1997), two limiting approaches were taken to consider the potential effect of soot surface oxidation of the O_2 that was present within the soot-containing region of all the present diffusion flames, as follows: (1) soot surface oxidation by the species under consideration was assumed to occur only by the collisional mechanism of Eqs. (6) and (7), and (2) the collisional mechanism was assumed to occur in parallel with an existing empirical soot surface oxidation mechanism involving O_2 due to Nagle and Strickland-Constable (1964), see Xu et al. (2003a) for a discussion of other O_2 oxidation mechanisms and the reasons why this particular choice was made.

The collision efficiencies of O_2 for soot surface oxidation at atmospheric pressure are plotted as a function of height above the burner exit in Fig. 10. Results shown on the figure include the range of values observed by Neoh et al. (1980,1984) in premixed flames, the values found from the present experiments in diffusion flames, (corrected for effects of soot surface growth) and values estimated using the empirical correlation for O_2 oxidation from Nagle and Strickland-Constable (1962) for the conditions where present measurements were made in diffusion flames. Note that the Nagle and Strickland-Constable (1962) correlation has proven to be effective for predicting soot surface oxidation by O_2, see Xu et al. (2003), and that there are significant concentrations of O_2 along the present soot paths, see Figs. 3-5. Thus, the fact that the Nagle and Strickland-Constable (1962) estimates of the O_2 collision efficiencies are 10 to 100 times smaller than the present measurements strongly suggests that some other species is mainly responsible for soot surface oxidation in the present flames. Other evidence that O_2 is not the main oxidizing species of soot for flame environments is provided by the large scatter (nearly a factor of 100) of the present O_2 collision efficiencies for diffusion flames combined with the even larger scatter of the O_2 collision efficiencies of Neoh et al. (1980,1984) for premixed flames.

The collision efficiencies of CO_2 for soot surface oxidation, are plotted as a function of height above the burner in Fig. 11. Results shown on the figure include the range of values observed by Neoh et al. (1980,1984) in premixed flames and values from the present investigation in diffusion flames at atmospheric pressure (corrected for effects of soot surface growth) both considering and ignoring the contribution of oxidation by O_2 (estimated using the Nagle and Strickland-Constable (1962) correlation). First of all, it is evident that allowing for direct soot surface oxidation by O_2 generally has only a small effect on the collision efficiencies estimated in Fig. 11. In addition, there is significant scatter (more than a factor of 10) of the

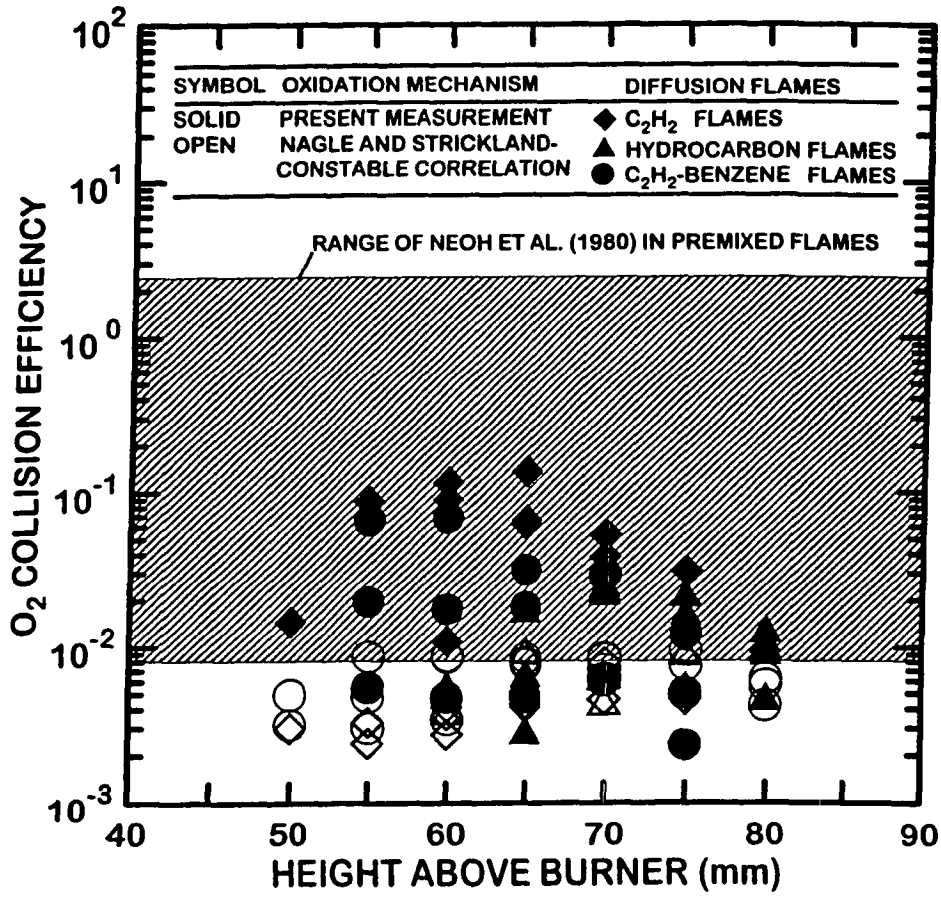

Fig. 10 Soot surface oxidation efficiencies assuming soot burnout due to attack by O_2 as a function of height above the burner. Found from the measurements of Neoh et al. (1980) in premixed flames, estimated from the correlation for attack by O_2 of Nagle and Strickland-Constable (1962) and from the measure- ments of Xu et al. (2003a) in diffusion flames. From Xu et al. (2003a).

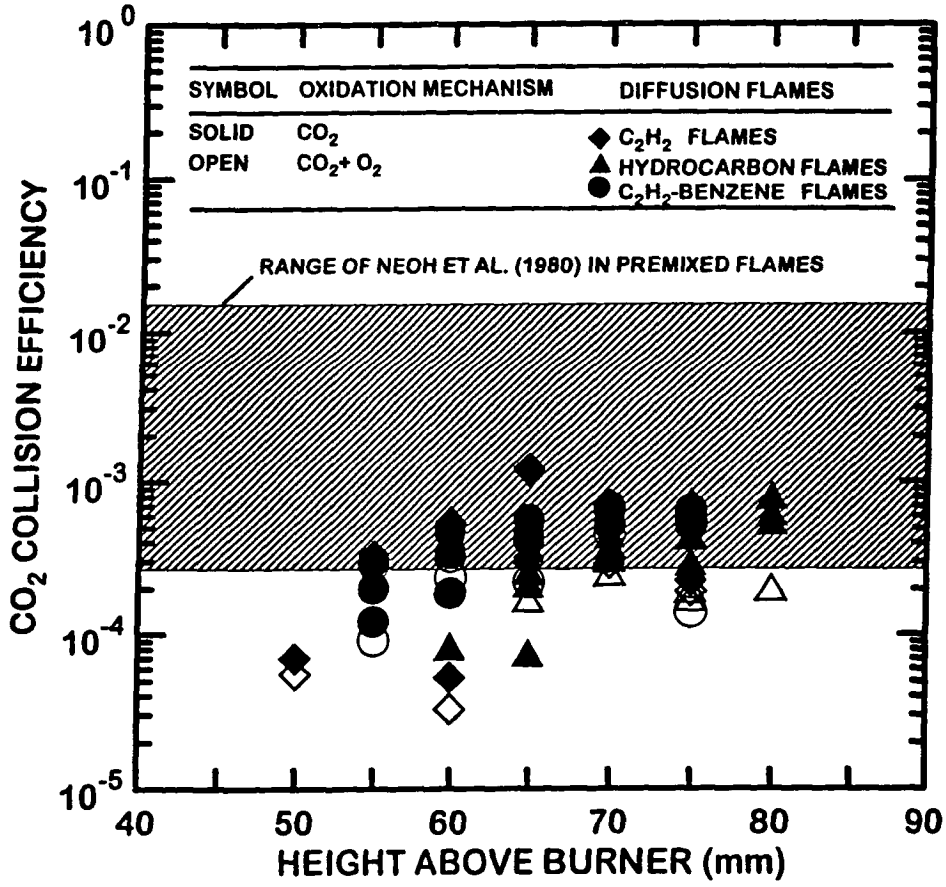

Fig. 11 Soot surface oxidation efficiencies assuming soot burnout due to attack by C O_2 as a function of height above the burner. Found from the measurements of Neoh et al. (1980) in premixed flames, estimated from the correlation for attack by O_2 of Nagle and Strickland-Constable (1962) and from the measurements of Xu et al. (2003a) in diffusion flames. From Xu et al. (2003a).

present collision efficiencies for CO_2 for diffusion flames, and even larger scatter (nearly a factor of 100) of the collision efficiences for CO_2 from Neoh et al. (1980,1984) for premixed flames. These findings clearly do not support CO_2 as a major direct contributor to soot surface oxidation in flame environments either alone or in parallel with soot surface oxidation by O_2.

Collision efficiencies for H_2O and O over the present premixed and diffusion flame data base also exhibited behavior similar to CO_2, see Xu et al. (2003). In particular, values of the collision efficiencies for these species scattered excessively for both the present measurements for diffusion flames and for the measurements of Neoh et al. (1980,1984) for premixed flames. In addition, the small concentrations of O in these flames required values of η_i in excess of unity, to explain observed soot oxidation rates, which clearly is not possible. These findings also do not support either H_2O or O as major direct contributors to soot surface oxidation in flame environments.

Finally, the collision efficiencies of OH for soot surface oxidation are plotted as a function of height above the burner in Fig. 12, in the same manner as the results for CO_2 in Fig. 11. With perhaps one exception, direct surface oxidation of soot by O_2 is not very important for these conditions, as before. On the other hand, similar to the observations of Neoh et al. (1980,1984) present collision efficiencies exhibit relatively small levels of scatter (roughly a factor of 3) compared to the other potential soot oxidizing species that have been considered. Furthermore, the results for premixed and diffusion flames in Fig. 12 are in remarkably good agreement with each other. In particular, the collision efficiency of OH for soot surface oxidation in the present diffusion flames is 0.14 with an uncertainty (95% confidence) of ± 0.04 after allowing for direct soot surface oxidation by O_2 using estimates from Nagle and Strickland-Constable (1962). This value is in excellent agreement with the value for soot surface oxidation from Neoh et al. (1980,1984) found from measurements of premixed flames of 0.13 with an uncertainty (95% confidence) of ± 0.03 when using the same treatment of soot structure and surface oxidation by O_2. In addition, direct effects of soot surface oxidation by O_2 were modest for present test conditions, with the OH collision efficiency only increasing from 0.14 to 0.17 when direct soot surface oxidation by O_2 was ignored. This behavior was achieved over a relatively broad range of flame conditions for the combined results in premixed and diffusion flames, as follows: temperatures of 1570-1870 K, oxygen (O_2) mole fractions of 1×10^{-5} - 3×10^{-2}, various hydrocarbon fuel types (acetylene, ethylene, propylene, propane and benzene) and levels of soot mass consumption less than 70% at atmospheric pressure. Although these results are helpful, the properties of the final stage of oxidation, where internal oxidation of primary particles becomes a factor, effects of pressures other than atmospheric pressure on soot surface oxidation , effects of high temperatures (> 1870 K, which are of interest for many practical applications) and additional consideration of effects of fuel type, e.g., fuels containing oxygen

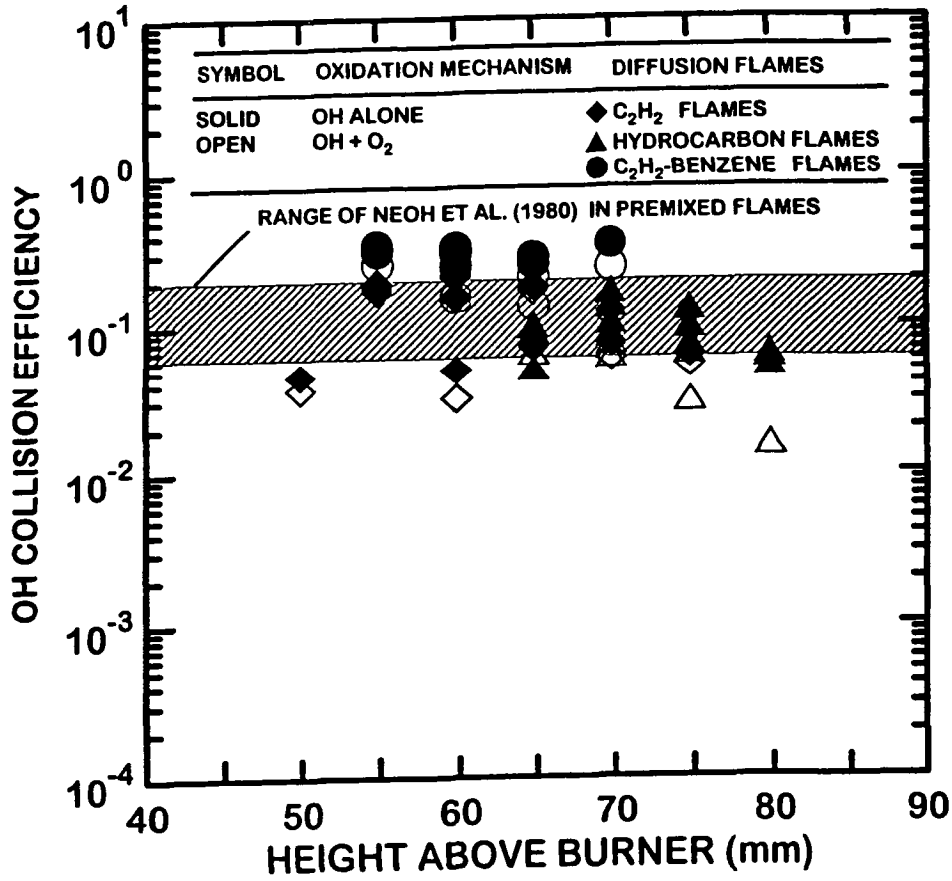

Fig. 12 Soot surface oxidation efficiencies assuming soot burnout due to attack by OH as a function of height above the burner. Found from the measurements of Neoh et al. (1980) in premixed flames, estimated from the correlation for attack by O_2 of Nagle and Strickland-Constable (1962) and from the measurements of Xu et al. (2003a) in diffusion flames. From Xu et al. (2003a).

would be of interest due to their potential to increase OH concentrations in the soot oxidation zone, all need to be considered in the future.

3.3 Conclusions

Soot surface growth and early soot surface oxidation were studied in coflowing buoyant laminar jet diffusion flames as summarized in Table 4: acetylene, ethylene, propylene, propane and benzene as fuels all burning air at atmospheric pressure and with all the reactants at normal temperature. In addition, the database for soot surface growth also included the measurements of Xu et al. (1997,1998) in premixed ethylene/air and methane/oxygen flames at atmospheric pressure. Finally, the database for early soot surface oxidation also included the measurements of Neoh et al. (1980,1984) for premixed ethylene/air flames at atmospheric pressure. Major conclusions of the study are as follows:

1) Soot surface growth rates in laminar premixed and diffusion flames, for various fuel and oxidant types, agree within experimental uncertainties at comparable local conditions and could be correlated reasonably well using the HACA soot surface growth mechanisms of Colket and Hall (1994), and Frenklach and Wang (1990,1994) and Kazakov et al. (1995)with the steric factors of both these mechanisms having values on the order of unity, as expected.

2) Measurements in the diffusion flames showed that significant degrees of soot formation begin near the jet exit once H first appears, in a prevailing condition where acetylene concentrations are relatively large, and that soot formation ends near the flame sheet where acetylene disappears in a prevailing condition where H concentrations are relatively large. This behavior is consistent with soot surface growth being dominated by the HACA mechanisms as noted in connection with conclusion 1. Finally, benzene was only observed for the benzene-fueled flames where benzene concentrations were both constant and relatively small (less than 1% by volume) throughout the soot formation region and were not particularly correlated with either the onset or the end of soot formation.

3) Potential soot surface oxidizing species in the region that was studied included O_2, CO_2, H_2O, O and OH; of these, only OH yielded a reasonable correlation of soot surface oxidation rates. Among the radical species, concentrations of O generally were much smaller than concentrations of OH throughout the soot surface oxidation region.

4) Present soot surface oxidation rates could be correlated by assuming a constant collision efficiency of OH of 0.14 with an uncertainty (95% confidence) of ± 0.04 after allowing for direct soot surface oxidation by O_2 using estimates from the Nagle and Strickland-Constable (1962) correlation; no significant effect of fuel type was observed for this behavior. This

finding also agreed within statistical significance with the earlier findings of Neoh et al. (1980,1984) in laminar premixed flames having similar concentrations of O_2.

5) The correction of present soot surface oxidation rates for oxidation by O_2, based on the results of Nagle and Strickland-Constable (1962) was small (e.g., the collision efficiency for OH only increased from 0.14 to 0.17 when soot surface oxidation by O_2 was ignored) compared to oxidation of OH for present conditions.

References

Bilger, R.W. (1976) "Turbulent Jet Diffusion Flames," *Prog. Energy Combust. Sci.* 1, 87-109.

Bockhorn, H., Fetting, F., Wannemacher, G. and Wentz, H. W. (1982) "Optical Studies of soot Particle Growth in Hydrocarbon Oxygen Flames," *Proc. Combust. Inst.* 19, 1413-1420.

Bockhorn, H., Fetting, F., Heddrich, A. and Wannemacher, G. (1984) "Investigation of the Surface Growth of Soot in Flat Low Pressure Hydrocarbon Oxygen Flames," *Proc. Combust. Inst.* 20, 979-988.

Colket, M.B. and Hall, R.J. (1994) "Successes and Uncertainties in Modelling Soot Formation in Laminar Premixed Flames," *Soot Formation in Combustion* (H. Bockhorn, ed.), Springer-Verlag, Berlin, pp. 442-470.

Dai, Z. and Faeth, G.M. (2000) "Hydrodynamic Suppression of Soot Formation in Laminar Coflowing Jet Diffusion Flames," *Proc. Combust. Inst.* 28, 2085-2092.

Dai, Z., Lin, K.-C., Sunderland, P.B., Xu, F. and Faeth, G.M. (1997) "Laminar Soot Processes (LSP)," Report No. GDL/GMF-97-01, Department of Aerospace Engineering, The University of Michigan, Ann Arbor, Michigan.

Dai, Z., El-Leathy, A.M., Lin, K.-C., Sunderland, P.B., Xu, F. and Faeth, G.M. (2000) "Laminar Soot Processes (LSP)," Report No. GDL/GMF 00-03, Department of Aerospace Engineering, The University of Michigan, Ann Arbor, Michigan.

El-Leathy, A.M. (2002) "*Effects of Hydrocarbon Fuel on Soot Surface Growth and Oxidation in Laminar Diffusion Flames*," Ph.D. Dissertation, Mechanical Power Department, Helwan University , Cairo, Egypt.

El-Leathy, A.M., Xu, F., Kim, C.H. and Faeth, G.M. (2003a) "Soot Surface Growth in Laminar Hydrocarbon/Air Diffusion Flames," *AIAA J.*, in press.

El-Leathy, A.M., Kim, C.H., Xu, F. and Faeth, G.M. (2003b) "Structure and Soot Reaction Properties of High-Temperature Diffusion Flames at Atmospheric Pressure," *AIAA J.*, in preparation.

Faeth, G.M. (1991) "Homogeneous Premixed and Nonpremixed Flames in Microgravity: A Review," *Proceedings of the AIAA/IKI Microgravity Science Symposium—Moscow,* AIAA, Washington, DC, pp. 281-293.

Faeth, G. M. (1997) "Combustion Fluid Dynamics (Tools and Methods)," in *Proc. Workshop on Fuels with Improved Fire Safety*, National Academy Press, Washington, DC, pp. 81-96.

Faeth, G.M. (2001) "Gaseous Laminar and Turbulent Diffusion Flames," *Microgravity Combustion Science* (H.D. Ross, editor), Academic Press, New York, pp. 83-182.

Faeth, G. M. and Köylü, Ü.Ö. (1995) "Soot Morphology and Optical Properties in Nonpremixed Turbulent Flame Environments," *Combust. Sci. Tech.* 108, 207-229.

Faeth, G.M. and Köylü, Ü.Ö. (1996) "Structure and Optical Properties of Flame-Generated Soot," *Transport Phenomena on Combustion* (S.H. Chan, ed.), Taylor & Francis, Washington, D.C., Vol. 1, pp. 19-44.

Frenklach, M. and Wang, H. (1990) "Detailed Modeling of Soot Particle Nucleation and Growth," *Proc. Combust. Inst.* 28, 1559-1556.

Frenklach, M. and Wang, H. (1994) "Detailed Mechanism and Modeling of Soot Particle Formation," *Soot Formation in Combustion* (H. Bockhorn, ed.), Springer-Verlag, Berlin, pp. 165-192.

Garo, A., Lahaye, J. and Prado, G. (1986) "Mechanisms of Formation and Destruction of Soot Particles in a Laminar Methane-Air Diffusion Flame," *Proc.Combust. Inst.* 21, 1023-1031.

Garo, A., Prado, G. and Lahaye, J(1990) "Chemical Aspects of Soot Particles Oxidation in a Laminar Methane-Air Diffusion Flame," *Combust. Flame* 79, 226-233.

Harris, S.J. and Weiner, A.M. (1983a) "Surface Growth of Soot Particles in Premixed Ethylene/Air Flames," *Combust. Sci. Tech.* 31, 155-167.

Harris, S.J. and Weiner, A.M. (1983b) "Determination of the Rate Constant for Soot Surface Growth," *Combust. Sci. Tech.* 32, 267-275.

Harris, S.J. and Weiner, A.M. (1984a) "Soot Particle Growth in Premixed Toluene/Ethylene Flames," *Combust. Sci. Tech.* 38, 75-87.

Harris, S.J. and Weiner, A.M. (1984b) "Some Constraints on Soot Particle Inception In Premixed Ethylene Flames," *Proc.Combust. Inst.* 20, 969-978.

Haudiquert, M., Cessou, A., Stepowski, D. and Coppalle, A. (1997) "OH and Soot Concentration Measurements in a High-Temperature Laminar Diffusion Flame," *Combust. Flame* 111:338-349.

Howard, J.B. (1990) "Carbon Addition and Oxidation Reactions in Heterogeneous Combustion and Soot Formation," *Proc.Combust. Inst.* 23, 1107-1127.

Kazakov, A.,Wang, H. and Frenklach, M. (1995) "Detailed Modeling of Soot Formation in Laminar Premixed Ethylene Flames at a Pressure of 10 Bar," *Combust. Flame* 110, 111-120.

Kim, C.H., El-Leathy, A.M., Xu, F. and Faeth, G.M. (2003) " Soot Surface Growth and Oxidation in Diffusion Flames at Subatmospheric and Atmosperic Pressures," *Combust. Flame*, in preparation.

Köylü, Ü.Ö. and Faeth, G.M. (1992) "Structure of Overfire Soot in Buoyant Turbulent Diffusion Flames at Long Residence Times," *Combust. Flame* 89, 140-156.

Köylü, Ü.Ö. and Faeth, G.M. (1993) "Radiative Properties of Flame-Generated Soot," *J. Heat Trans.* 115, 409-417.

Köylü, Ü.Ö. and Faeth, G.M. (1994a) "Optical Properties of Overfire Soot in Buoyant Turbulent Diffusion Flames at Long Residence Times," *J. Heat Trans.* 116, 152-159.

Köylü, Ü.Ö. and Faeth, G.M. (1994b) "Optical Properties of Soot in Buoyant Laminar Diffusion Flames," *J. Heat Trans.* 116, 971-979.

Köylü, Ü.Ö. and Faeth, G.M. (1996) "Spectral Extinction Coefficients of Soot Aggregates from Turbulent Diffusion Flames," *J. Heat Trans.* 118, 415-421.

Köylü, Ü.Ö., Faeth, G.M., Farias, T.L. and Carvalho, M.G. (1995) "Fractal and Projected Structure Properties of Soot Aggregates," *Combust. Flame* 100, 621-633.

Krishnan, S.S., Lin, K.-C. and Faeth, G.M., (2000) "Optical Properties in the Visible of Overfire Soot in Large Buoyant Turbulent Diffusion Flames," *J. Heat Trans.* 122, 517-524.

Krishnan, S.S., Lin, K.-C., and Faeth, G.M. (2001) "Extinction and Scattering Properties of Soot Emitted from Large Buoyant Turbulent Diffusion Flames," *J. Heat Trans.* 123, 331-339.

Law, C.K. and Faeth, G.M. (1994) "Opportunities and Challenges of Combustion in Microgravity," *Prog. Energy Combust. Sci.* 20, 65-113.

Leung, K.M. and Lindstedt, R.P. (1995) "Detailed Kinetic Modeling of C_1-C_3 Alkane Diffusion Flames," *Combust. Flame* 102, 129-160.

Leung, K.M., Lindstedt, R.P. and Jones, W.P. (1991) "A Simplified Reaction Mechanism for Soot Formation in Nonpremixed Flames," *Combust. Flame* 87, 289-305.

Lin, K.-C. and Faeth, G.M. (1998) "Shapes of Nonbuoyant Round Luminous Hydrocarbon/Air Laminar Jet Diffusion Flames," *Combust. Flame* 116, 415-431

Lin, K.-C. and Faeth, G.M. (2000) "State Relationships of Laminar Permanently-Blue Opposed-Jet Hydrocarbon-Fueled Diffusion Flames," *Int. J. Environ. Combust. Tech.* 1, 53-79.

Lin, K.-C., Sunderland, P.B. and Faeth, G.M. (1996) "Soot Nucleation and Growth in Acetylene/Air Laminar Coflowing Jet Diffusion Flames," *Combust. Flame* 104, 369-375.

Maus, F., Schäfer, T. and Bockhorn, H. (1994) "Inception and Growth of Soot Particles in Dependence of the Surrounding Gas Phase," *Combust. Flame* 99, 697-705.

Nagle, J. and Strickland-Constable, R.F. (1962) "Oxidation of Carbon Between 1000-2000 °C," *Proceedings of Fifth Carbon Conference*, Vol. 1, 154-164.

Neoh, K.G., Howard, J.B. and Sarofim, A.F. (1980) "Soot Oxidation in Flames," *Particulate Carbon* (D.C. Siegla and B.W. Smith, ed.), Plenum Press, New York, pp. 261-277.

Neoh, K.G., Howard, J.B. and Sarofim, A.F. (1984) "Effect of Oxidation on the Physical Structure of Soot," *Proc. Combust. Inst.* 20, 951-957.

Ramer, E.R., Merklin, J.F., Sorensen, C.M. and Taylor, T.W. (1986) "Chemical and Optical Probing of Premixed Methane/Oxygen Flames," *Combustion Science and Technology*, 48, 241-255.

Sunderland, P.B. and Faeth, G.M. (1996) "Soot Formation in Hydrocarbon/Air Laminar Jet Diffusion Flames," *Combust. Flame* 105, 132-146.

Sunderland, P.B., Mortazavi, S., Faeth, G.M. and Urban, D.L. (1994) "Laminar Smoke Points of Nonbuoyant Jet Diffusion Flames," *Combust. Flame* 96, 97-103.

Sunderland, P.B., Köylü, Ü.Ö. and Faeth, G.M. (1995) "Soot Formation in Weakly Buoyant Acetylene-Fueled Laminar Jet Diffusion Flames Burning in Air," *Combust. Flame* 100, 310-322.

Urban, D.L., Yuan, Z.-G., Sunderland, P.B., Linteris, G.T., Voss, J.E., Lin, K.-C., Dai, Z., Sun, K. and Faeth, G.M. (1998) "Structure and Soot Properties of Nonbuoyant Ethylene/Air Laminar Jet Diffusion Flames,"*AIAA J.* 36, 1346-1360.

Urban, D.L., Yuan, Z.-G., Sunderland, P.B., Lin, K.-C., Dai, Z. and Faeth, G.M. (2000) "Smoke-Point Properties of Nonbuoyant Round Laminar Jet Diffusion Flames," *Proc. Combust. Inst.* 28, 1965-1972.

Wieschnowsky, U., Bockhorn, H. and Fetting, F. (1988) "Some New Observations Concerning the Mass Growth of Soot in Premixed Hydrocarbon/Oxygen Flames," *Proc. Combust. Inst.* 22, 343-352.

Xu, F. and Faeth, G.M. (2000) "Structure of the Soot Growth Region of Laminar Premixed Methane/Oxygen Flames," *Combust. Flame* 121, 640-650

Xu, F. and Faeth, G.M. (2001) "Soot Formation in Laminar Acetylene/Air Diffusion Flames at Atmospheric Pressure," *Combust. Flame* 125, 804-819.

Xu, F., Sunderland, P.B. and Faeth, G.M. (1997) "Soot Formation in Laminar Premixed Ethylene/Air Flames at Normal Temperature and Pressure," *Combust. Flame* 108, 471-493.

Xu, F., Lin, K.-C. and Faeth, G.M. (1998) "Soot Formation in Laminar Premixed Methane/Oxygen Flames at Atmospheric Pressure," *Combust. Flame* 115, 195-209.

Xu, F., Dai, Z. and Faeth, G.M. (2002) "Flame Shapes of Nonbuoyant Laminar Jet Diffusion Flames," *AIAA J.*, 40, 2439-2446.

Xu, F., El-Leathy, A.M., Kim, C.-H. and Faeth, G.M. (2003) "Soot Surface Oxidation in Laminar Hydrocarbon/Air Diffusion Flames at Atmospheric Pressure," *Combust. Flame*, in press.